Supporting Information

Photoactivated Hydride Therapy under Hypoxia beyond ROS

Xia Wang,‡[a] Yijian Gao,‡[b] Ting Wang,[c] Zhaobin Wang,[a] He Hang,[a] Shengliang Li,*[b]

Fude Feng*[a]

[a] MOE Key Laboratory of High Performance Polymer Material and Technology of Ministry of Education, Department of Polymer Science & Engineering, School of Chemistry & Chemical Engineering, Nanjing University, Nanjing 210023, China

[b] College of Pharmaceutical Sciences, Soochow University, Suzhou 215123, China

[c] State Key Laboratory of Analytical Chemistry for Life Science, School of Chemistry and Chemical Engineering, Nanjing University, Nanjing 210023, China

‡ These authors contributed equally to this work.

Experimental methods

Chemicals and materials

All chemical reagents and solvents were purchased from commercial sources and used without further purification unless otherwise described.

Characterization methods

^{1}H NMR and ^{13}C NMR spectra were characterized by nuclear magnetic resonance (NMR) spectrometer (Bruker, ARX-400 MHz). High-resolution mass spectra (HRMS) were performed using an electrospray Agilent Q-TOF mass spectrometer system (Q-TOF-6540). Ultraviolet-visible (UV-vis) absorption spectra were obtained on a UV-vis spectrophotometer (Shimadzu, UV-2600). Fluorescence spectra were measured on Hitachi F-7000 fluorimeter. Fluorescence lifetimes were measured on a steady state and transient state fluorescence spectrometer (Edinburgh, FLS980). Fluorescent cell images were acquired by a confocal laser scanning microscope (CLSM, Q2, ISS Inc., Italy) and an inverted fluorescence microscope (Nikon, TE2000-U, Japan).

Synthesis and characterization

Synthesis of Por-1

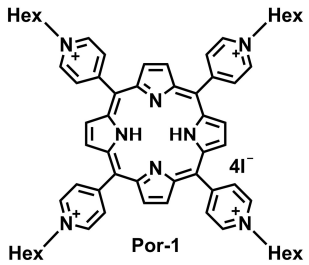

Por-1

5,10,15,20-Tetra(4-pyridyl)porphyrin (92.7 mg, 0.15 mmol) and 1-iodohexane (878 μL, 6 mmol) were dissolved in anhydrous DMF (10 mL). The mixture was stirred at 140 °C for 12 h. The reaction mixture was cooled and the product precipitated was washed with diethyl ether. After drying under vacuum, dark violet solid product (187.2 mg, 85%) was obtained. ^{1}H NMR (400 MHz, DMSO-d_6) δ (ppm): 9.61 (d, J =6.4 Hz, 8H), 9.27 (s, 8H), 9.05 (d, J =6.4 Hz, 8H), 4.98 (t, J =7.2 Hz, 8H), 2.32 (m, 8H), 1.63 (m, 8H), 1.49 (m, 16H), 1.00 (t, J =6.8 Hz, 12H), -3.07 (s, 2H). ^{13}C NMR (100 MHz, DMSO-d_6) δ (ppm): 156.91, 143.95, 133.00, 116.37, 61.36, 31.42, 31.33, 25.94, 22.50, 14.45. HRMS (ESI+): m/z 239.6585 [M/4], 291.1766 [(M-C_6H_{13})/3], 319.2077 [(M-H)/3].

Synthesis of Por-2 (TMPyP)

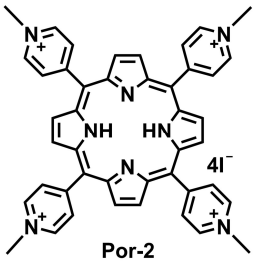

Por-2

5,10,15,20-Tetra(4-pyridyl)porphyrin (92.7 mg, 0.15 mmol) and methyl iodide (560 μL, 9 mmol) were dissolved in anhydrous DMF (10 mL). The mixture was stirred at 140 °C for 12 h. The purification procedure was carried out as described for the synthesis of Por-1. Dark violet solid product (147.8 mg, 83%) was obtained. ^{1}H NMR (400 MHz, DMSO-d_6) δ (ppm): 9.49 (d, J =6.4 Hz, 8H), 9.21 (s, 8H), 9.00 (d, J =6.4 Hz, 8H), 4.73 (s, 12H), -3.09 (s, 2H). ^{13}C NMR (100 MHz, DMSO-d_6) δ (ppm): 156.18, 144.24, 132.07, 115.82, 47.92. HRMS (ESI+): m/z 169.5804 [M/4], 221.0986 [(M-CH_3)/3], 226.1055 [M/3].

Synthesis of Por-3

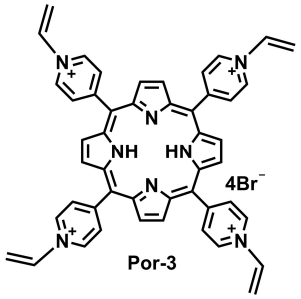

Por-3

5,10,15,20-Tetra(4-pyridyl)porphyrin (92.7 mg, 0.15 mmol) and allyl bromide (779 μL, 9 mmol) were dissolved in anhydrous DMF (10 mL). The mixture was stirred at 140 °C for 12 h. The reaction mixture was cooled and the product precipitated was washed with acetone. After drying under vacuum, dark violet solid product (132.1 mg, 80%) was obtained. ^{1}H NMR (400 MHz, DMSO-d_6) δ (ppm): 9.58 (d, J =6.8 Hz, 8H), 9.27 (s, 8H), 9.07 (d, J =6.8 Hz, 8H), 6.53 (m, 4H), 5.86 (d, J =17.1 Hz, 4H), 5.74-5.69 (m, 12H), -3.07 (s, 2H). ^{13}C NMR (100 MHz, DMSO-d_6) δ (ppm): 156.77, 143.48, 132.61, 131.67, 122.73, 115.85, 62,45. HRMS (ESI+): m/z 195.5955 [M/4], 247.1151 [(M-C_3H_5)/3], 260.4584 [(M-H)/3], 350.1515 [(M-2C_3H_5)/2].

Synthesis of Por-4

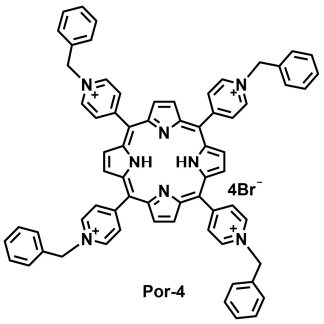

Por-4

5,10,15,20-Tetra(4-pyridyl)porphyrin (92.7 mg, 0.15 mmol) and benzyl bromide (713 μL, 6 mmol) were dissolved in anhydrous DMF (10 mL). The mixture was stirred at 140 °C for 12 h. The purification procedure was carried out as described for the synthesis of Por-1. Dark violet solid product (151.5 mg, 78%) was obtained. ^{1}H NMR (400 MHz, DMSO-d_6) δ (ppm): 9.73 (d, J =6.8 Hz, 8H), 9.25 (s, 8H), 9.07 (d, J =6.7 Hz, 8H), 7.95 (d, J =6.9 Hz, 8H), 7.67-7.58 (m, 12H), 6.30 (s, 8H), -3.08 (s, 2H). ^{13}C NMR (100 MHz, DMSO-d_6) δ (ppm): 156.81, 143,56, 134,02, 132.89, 129.62, 129.57, 129.34, 115.82, 63.20. HRMS (ESI+): 297.1297 [(M-C_7H_7)/3], 327.1461 [(M-H)/3], 400.1683 [(M-2C_7H_7)/2].

Synthesis of ZnPor

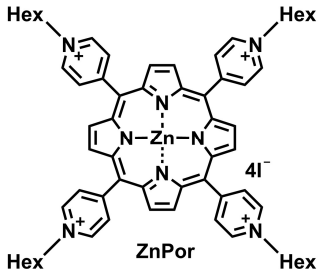

ZnPor

The mixture of Por-1 and $ZnCl_2$ (20 eq.) dissolved in ethanol-water (v/v = 4: 1) was heated to reflux. The reaction was monitored by UV-vis spectrometry. After the reaction was completed, solvent was removed under vacuum. The product precipitated by acetone was filtered and washed with acetone, diethyl ether, and acetone, respectively. Dark violet solid product was obtained. ^{1}H NMR (400 MHz, DMSO-d_6) δ (ppm): 9.53 (d, J =6.5 Hz, 8H), 9.09 (s, 8H), 8.93 (d, J =6.5 Hz, 8H), 4.96 (t, J =7.2 Hz, 8H), 2.29 (m, 8H), 1.61 (m, 8H), 1.47 (m, 16H), 0.99 (t, J =6.8 Hz, 12H).

Synthesis of ZnTAPP

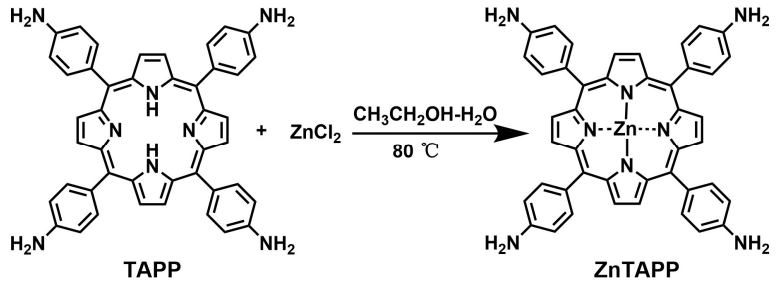

Scheme S1 Synthetic route of ZnTAPP.

ZnTAPP was prepared from TAPP according to the previous procedure.[1]

Synthesis of ^{mito}Por and ^{mito}ZnPor

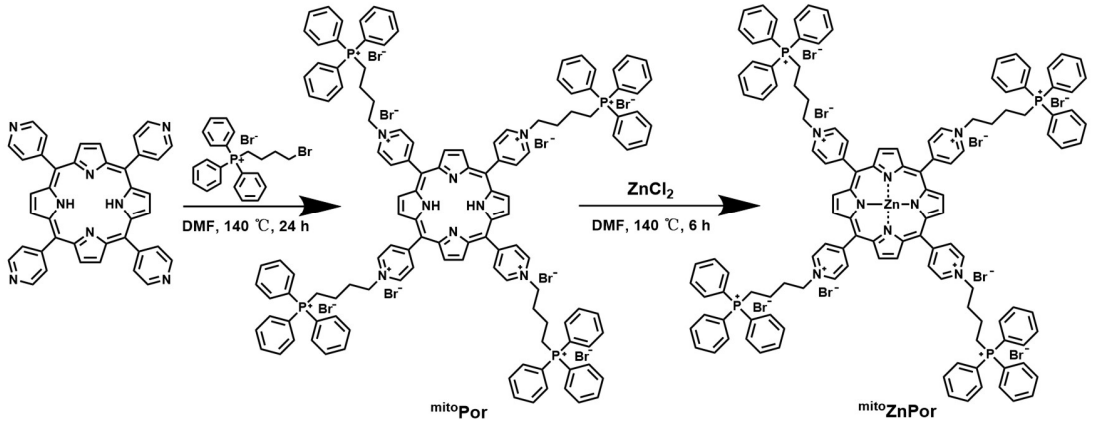

Scheme S2 Synthetic route of ^{mito}Por and ^{mito}ZnPor.

5,10,15,20-Tetra(4-pyridyl)porphyrin (61.8 mg, 0.1 mmol) and (4-bromobutyl)triphenylphosphonium bromide (1428.0 mg, 3 mmol) were dissolved in anhydrous DMF (10 mL). The mixture was stirred at 140 °C for 24 h. Then the mixture was cooled and the product precipitated was washed with diethyl ether and dichloromethane (v/v = 1: 1). After drying under vacuum, dark violet solid product (^{mito}Por) (110.8 mg, 44%) was obtained. ^{1}H NMR (400 MHz, DMSO-d_6) δ (ppm): 9.67 (d, J =6.1 Hz, 8H), 9.27 (s, 8H), 9.05 (d, J =6.1 Hz, 8H), 7.94 (m, 36H), 7.85 (m, 24H), 5.11 (t, J =7.2 Hz, 8H), 4.01 (m, 8H), 2.55 (t, J =5.5 Hz, 8H), 1.93 (m, 8H), -3.07 (s, 2H). ^{13}C NMR (100 MHz, DMSO-d_6) δ (ppm): 156.46, 143,51, 135.05, 133.81, 133.70, 132.50, 130.41, 130.28, 118.84, 117.98, 115.87, 59.42, 34.26, 20.38, 18.95. HRMS (ESI+): 236.4796 [M/8], 262.2809 [(M-$C_{22}H_{23}$)/6], 270.1186 [(M-H)/7], 314.9688 [(M-2H)/6], 377.7631 [(M-3H)/5].

The mixture of ^{mito}Por (50.8 mg, 0.02 mmol) and $ZnCl_2$ (54.5 mg, 0.4 mmol) dissolved in anhydrous DMF (5 mL) was heated at 140 °C for 6 h. The reaction was monitored by UV-vis spectrometry. After the reaction was completed, the mixture was precipitated with ethyl ether to obtain ^{mito}ZnPor as a solid product (46.9 mg, 90%). ^{1}H NMR (400 MHz, DMSO-d_6) δ (ppm): 9.52

(d, J =6.2 Hz, 8H), 9.10 (s, 8H), 8.95 (d, J =6.2 Hz, 8H), 7.95 (m, 36H), 7.85 (m, 24H), 5.03 (t, J =6.0 Hz, 8H), 3.91 (m, 8H), 2.56 (m, 8H), 1.91 (m, 8H). HRMS (ESI+): 244.3443 [M/8], 272.7666 [(M-$C_{22}H_{23}$)/6], 284.2467 [(M+ Cl)/7], 326.9186 [(M-H-$C_{22}H_{23}$)/5].

Isothermal titration calorimetry (ITC) experiment

The ITC measurements were conducted on a MicroCal^{TM} iTC_{200} with a stainless steel sample cell at 25.00 ± 0.01 °C. The sample cell was initially loaded with 350 μL of 0.2 mM porphyrin solution (10% DMSO/1× pH 7.4 PBS), and then NADH solution (8 mM in 10% DMSO/1× pH 7.4 PBS) was injected into the stirred sample cell in portions of 2 μL until the end of the interaction. As dilution of DMSO can induce energy response, the standard dilution enthalpy of solvent mixing in an independent experiment has been deducted before the curve was fitted properly.

Reactivity of cPor/ZnPor towards NADH

After light irradiation (λ 405 nm, 25 mW cm^{-2}) for certain periods, the solutions containing cPor/ZnPor (20 μM) and NADH (200 μM) in deoxygenated pH 7.4 PBS were monitored by UV-vis absorption spectroscopy. In a parallel experiment, the reactions between Por-1/ZnPor (20 μM), NADH (200 μM) and TEMPO (10 mM) after light treatment in deoxygenized pH 7.4 PBS were measured by UV-vis absorption spectra after light treatment.

Cyclic voltammetry measurement

The cyclic voltammetry measurement was performed in degassed PBS containing ZnPor (0.1 mM) and NADH (1 mM) pre and post irradiation. Cyclic voltammograms was recorded pre and post irradiation (white LED lamp, 30 mW cm^{-2}). Experimental conditions: reference electrode, Ag/AgCl; working electrode, glassy carbon; auxiliary electrode, Pt; temperature, 298 K; scan rate, 100 mV/s.

Ultrahigh performance liquid chromatography (UPLC) analysis

For the degassed PBS solution containing ZnPor (20 μM) and NADH (200 μM) pre and post light irradiation (λ 405 nm, 25 mW cm^{-2}), UPLC was used to monitor the reaction process upon different wavelength channel (440, 530, 799 nm). Then, after the irradiated solution was exposed to oxygen, the solution was further analyzed by UPLC.

Reactivity of ZnTAPP towards NADH

In deoxygenized 30% THF/pH 7.4 PBS, the solutions containing TAPP or ZnTAPP (20 μM) and NADH (200 μM) were irradiated with LED light (λ 405 nm, 25 mW cm^{-2}) for certain periods. The UV-vis absorption spectra were collected to monitor the reaction process.

The reactivity of ZnPhl to different oxidative species

In deoxygenated pH 7.4 PBS, the cuvette containing ZnPor (10 μM) and NADH (200 μM) was irradiated with LED light (λ 405 nm, 25 mW cm^{-2}) for 10 s to obtain ZnPhl. Then oxidative species was added into solutions quickly containing ZnPhl, then the cuvette was shaken rapidly. The UV-vis absorption spectra were collected to monitor the absorption change.

The final concentration of oxidative species: MB 10 μM, para-quinone 100 μM, p-chloranil 100 μM, GSH 1 mM, NAD^+ 1 mM, CoQ10 100 μM, hemin 20 μM, Cyt c_{ox} 0.1 mg mL^{-1}, H_2O_2 2 mM, $OH^•$ (H_2O_2 0.5 mM + HRP 2 μg mL^{-1}), respectively.

ZnPor/ZnPhl-based photochemical experiment on MB/Cyt c_{ox}

After light irradiation (λ 405 nm, 25 mW cm^{-2}), the solutions containing ZnPor (1 μM), NADH (100 μM) and MB (10 μM)/Cyt c_{ox} (0.1 mg mL^{-1}) in deoxygenated pH 7.4 PBS were measured by UV-vis absorption spectroscopy. The TOF toward Cyt c_{ox} was calculated using the extinction coefficient ε_{550} = 28000 $M^{-1}cm^{-1}$ in PBS buffer.[2]

Photochemical experiment on Cyt c_{ox} using ^{mito}Por and ^{mito}ZnPor

After light irradiation (λ 405 nm, 25 mW cm^{-2}), the solutions containing ^{mito}Por/^{mito}ZnPor (1 μM), NADH (50 μM) and Cyt c_{ox} (0.1 mg mL^{-1}) in deoxygenated PBS (pH 7.4) were measured by UV-vis absorption spectra.

Photochemical experiment on CoQ10 using ^{mito}Por and ^{mito}ZnPor

After light irradiation (λ 405 nm, 25 mW cm^{-2}) for 5 min, the mixture containing ^{mito}Por (1μM) /^{mito}ZnPor (2 μM), NADH (100 μM) and CoQ10 (50 μM) in deoxygenated PBS (pH 7.4) was diluted by 10 times with acetonitrile and subjected to HRMS measurement. In a parallel experiment, CoQ10 (100 μM) was added to the solution containing ^{mito}Phl/ ^{mito}ZnPhl to collect the UV-vis absorption.

Cell culture

The cell lines HeLa, A549, HepG2, L02, RAW264.7 were purchased from Jiangsu KeyGEN Biotechnology Corp., Ltd. The cell lines 4T1, QSG, HPNE, bEnd.3 were purchased from Wuhan Pricella Biotechnology Corp., Ltd. U87MG cells were purchased from Center for Excellence in Molecular Cell Science, CAS. All cells were cultured in DMEM medium supplemented with 10% fetal bovine serum (WISENT BioTECH Corp., Ltd) at 37 °C in a humidified incubator with 5% CO_2.

Confocal fluorescence imaging

A549 cells were seeded in 4-well glass-bottomed plates (Φ = 40 mm) at a density of 8×10^4 cells per well and cultured for 24 h. The cells were incubated with ^{mito}ZnPor (4 μM) for 4 h, and then

incubated with Mitochondria green tracker (0.1 μM) for 1 h. After washing with PBS, the cells were performed CLSM imaging. ^{mito}ZnPor: excited at 405 nm, emission collected at 600-700 nm. Mitochondria green tracker: excited at 488 nm, emission collected at 500-600 nm.

MTT assay

Cancer cells (HeLa, 4T1, U87MG, A549, HepG2) or normal cells (L02, QSG, HPNE, bEnd.3) or macrophages (RAW264.7) were seeded in 96-well plates and incubated for 24 h under a humidified atmosphere at 37 °C and 5% CO_2. For the irradiation group, the cells were incubated in the fresh growth medium containing ^{mito}ZnPor at different concentrations for 4 h in hypoxic (1% O_2) atmosphere. Then the cells were exposed to light irradiation for 10 min with a white LED lamp (30 mW cm^{-2}). The cells continued to incubate for 24 h in dark. For dark treatment group, the cells were treated with ^{mito}ZnPor in hypoxic (1% O_2) and dark atmosphere for the same time as the irradiation group. Then the medium was replaced by 100 μL of fresh medium containing MTT (0.1 mg mL^{-1}) and the cells were incubated at 37 °C for 3 h. The medium was carefully removed and DMSO (100 μL) was added to dissolve the formazan in cells. Finally, the absorption intensity at 560 nm was recorded with a Tecan multimode microplate reader to evaluate the cell viability of drugs at different concentrations.

MTT assay with supplement of exogenous NADH

L02 or HepG2 cells were seeded in 96-well plates and incubated for 24 h under a humidified atmosphere at 37 °C and 5% CO_2. The cells were incubated with NADH (1 mM) for 2 h, then the cells were incubated in the fresh growth medium containing ^{mito}ZnPor at different concentrations for 4 h in hypoxic (1% O_2) atmosphere. For the irradiation group, the cells were exposed to light irradiation for 10 min with a white LED lamp (30 mW cm^{-2}) and continued to incubate for 24 h in dark. For dark treatment group, the cells were in hypoxic (1% O_2) and dark atmosphere for the same time as the irradiation group. Finally, the cell viability was evaluated as described above.

MTT assay with ROS scavenger

Cancer cells (HeLa, 4T1, A549) were seeded in 96-well plates at a density of 2×10^4 cells per well and incubated for 24 h under a humidified atmosphere at 37 °C and 5% CO_2. The cells were incubated with NaAA (1 mM) or NAC (1 mM) or NaN_3 (10 mM) for 1 h, then the cells were incubated in the fresh growth medium containing ^{mito}ZnPor at different concentrations for 4 h in hypoxic (1% O_2) atmosphere. For the irradiation group, the cells were exposed to light irradiation for 10 min with a white LED lamp (30 mW cm^{-2}) and continued to incubate for 24 h in dark. For dark treatment group, the cells were in hypoxic (1% O_2) and dark atmosphere for the same time as the irradiation group. Finally, the cell viability was evaluated as described above.

Live/Dead cell staining

A549 cells were seeded in 96-well plates and incubated for 24 h at 37 °C and 5% CO_2. After the cells were treated with various concentrations of ^{mito}ZnPor for 4 h in hypoxic (1% O_2) atmosphere, the cells were irradiated with a white LED lamp (30 mW cm^{-2}) for 10 min, followed by another 24 h of incubation at 37 °C**.** After removal of the medium, the cells were incubated with Calcein-AM/ PI double stain kit according to the instruction manual, then the cells were imaged on an inverted fluorescent microscope.

Co-cultured model treated with ^{mito}ZnPor

Cancer cells and normal cells (or macrophages) were seeded in 96-well plates together and co-incubated for 24 h at 37 °C and 5% CO_2. The cells were incubated in the fresh growth medium containing ^{mito}ZnPor (0, 1 or 2 μM) for 4 h in hypoxic (1% O_2) atmosphere. Then the cells were exposed to light irradiation for 10 min with a white LED lamp (30 mW cm^{-2}) and continued to incubate for 48 h in dark.

For the co-cultured model of HepG2 and L02 cells or A549 and RAW264.7 cells, the cells were incubated with Calcein-AM/PI double stain kit according to the instruction manual after treated as described above, then the cells were observed by an inverted fluorescence microscope.

For the co-cultured model of HepG2 and L02 cells, the cells were stained with 100 μL of trypan blue stain (0.4%) for 5 min after treated as described above, then the cells were observed by an inverted fluorescence microscope.

For the co-cultured model of HepG2 and L02 cells, the cells were rinsed with PBS carefully after treated as described above, then continued to incubate for 48 h. The cells were observed by an inverted fluorescence microscope.

Co-cultured model treated with Ce6

HepG2 and L02 cells or A549 and RAW264.7 cells were seeded in 96-well plates together and co-incubated for 24 h at 37 °C and 5% CO_2. The cells were incubated in the fresh growth medium containing Ce6 (0, 1 or 2 μM) for 4 h in hypoxic (1% O_2) atmosphere. Then the cells were exposed to light irradiation for 10 min with a white LED lamp (30 mW cm^{-2}) and continued incubation for 48 h in dark. After incubation with Calcein-AM/PI double staining kit according to the instruction manual, the cells were imaged by an inverted fluorescence microscope.

Two-photon fluorescence imaging

HeLa cells were seeded in 4-well glass-bottomed plates (Φ = 40 mm) at a density of 8×10^4 cells per well and cultured for 24 h. Then the cells were treated with ^{mito}ZnPor (4 μM) for 4 h, and washed with PBS, followed by addition of fresh growth medium. Two-photon fluorescence imaging was

performed with a Leica TCS SP5 laser scanning microscope with a 20× objective lens. Samples were excited by an 800 nm Ti-Sapphire laser, with emission collected between 600 and 700 nm.

Measurement of intracellular NADH concentration

HeLa cells were seeded in 12-well plates at a density of 6×10^5 cells per well and incubated for 24 h. Then the cells were treated with various concentrations of ^{mito}ZnPor (0, 0.125, 0.25, 0.5, 2 μM) for 4 h in hypoxic (1% O_2) atmosphere. After light irradiation for 10 min (λ 405 nm, 30 mW cm^{-2}) and another 10 h of incubation at 37 °C, the NAD^+/NADH Assay Kit (Beyotime Biotechnology) was used to measure the intracellular NADH concentration according to the instruction manual.

Measurement of intracellular SDH activity

HeLa cells were seeded in petri dishes at a density of 3×10^6 cells and incubated for 24 h. Then the cells were treated with various concentrations of ^{mito}ZnPor (0, 0.125, 0.5, 1 μM) for 4 h in hypoxic (1% O_2) atmosphere. After light irradiation (white LED lamp, 30 mW cm^{-2}) for 10 min, the SDH Activity Assay Kit (Solarbio Science & Technology) was used to measure the intracellular SDH activity according to the instruction manual.

Measurement of intracellular ATP concentration

HeLa cells were seeded in 24-well plates and incubated for 24 h. Then the cells were treated with various concentrations of ^{mito}ZnPor (0, 0.125, 0.25, 0.5, 2 μM) for 4 h in hypoxic (1% O_2) atmosphere. After light irradiation for 10 min (λ 405 nm, 30 mW cm^{-2}) and another 10 h of incubation at 37 °C, the ATP Assay Kit (Beyotime Biotechnology) was used to measure the intracellular ATP concentration according to the instruction manual.

Formazan formation assay

HeLa or L02 cells were seeded in 96-well plates and incubated for 24 h under a humidified atmosphere at 37 °C and 5% CO_2. Then the cells were incubated in the fresh growth medium containing ^{mito}ZnPor (0 or 2 μM) for 4 h in hypoxic (1% O_2) atmosphere. After light irradiation for 10 min with a white LED lamp (30 mW cm^{-2}), MTT solutions (20 μL, 5 mg/mL) in PBS were added to each well. After incubated for another 4 h at 37 °C, the cells were imaged by an inverted fluorescence microscope.

Intracellular ROS measurement

2′,7′-dichlorodihydrofluorescein diacetate (DCFH-DA) was used to evaluate intracellular ROS generation under normoxia and hypoxia.[3]

For normoxia treatment, HeLa cells were seeded in 96-well plates and incubated for 24 h. Then the cells were treated with ^{mito}ZnPor (1 μM) for 4 h. After light irradiation (white LED lamp, 30

mW cm^{-2}) for 10 min, the cells were incubated with DCFH-DA (10 μM) for 30 min. Then the cells were rinsed with PBS for 2 times, followed imaged by an inverted fluorescence microscope.

For hypoxia treatment, HeLa cells were seeded in 96-well plates and incubated for 24 h. Then the cells were treated with ^{mito}ZnPor (1 μM) for 4 h in hypoxic (1% O_2) atmosphere and irradiated (white LED lamp, 30 mW cm^{-2}) for 10 min. After the cells were incubated with DCFH-DA (10 μM) for 30 min and rinsed with PBS for 2 times, fluorescence images were observed by an inverted fluorescence microscope.

Lipid peroxidation (LPO) detection

For LPO detection, C11- BODIPY$^{581/591}$ was used to assess the intracellular LPO level. HeLa cells were seeded in a 40 mm 4-well glass-bottomed plate for 24 h. Then the cells were treated with various concentrations of ^{mito}ZnPor (0, 0.25, 0.5, 2 μM) for 4 h in hypoxic (1% O_2) atmosphere. Photoirradiation was proceeded with a white LED lamp (30 mW cm^{-2}) for 10 min, and then HeLa cells were stained with C11-BODIPY (5 μM) for 30 min before confocal fluorescence imaging (λ_{ex} = 488 nm; λ_{em} = 495-540 nm).

For the control group, HeLa cells were treated with TAPP (4 μM) for 4 h in normoxia (21% O_2) atmosphere, then the cells were irradiated for 10 min (λ 405 nm, 30 mW cm^{-2}). After light irradiation, HeLa cells were incubated with C11-BODIPY (5 μM) for 30 min before confocal fluorescence imaging (λ_{ex} = 488 nm; λ_{em} = 495-540 nm).

JC-1 assay

JC-1 dye was employed to detect the mitochondrial membrane potential. HeLa or L02 cells were seeded in a 40 mm 4-well glass-bottomed plate at a density of 1×10^5 cells per well for 24 h. Then the cells were treated with ^{mito}ZnPor (0 or 1 μM) for 4 h in hypoxic (1% O_2) atmosphere. After light irradiation (white LED lamp, 30 mW cm^{-2}) for 10 min, the cells were stained with JC-1 for 20 min at 37 °C and washed with PBS. Finally, the cells were subjected to CLSM imaging. Green fluorescence channel: λ_{ex} = 488 nm, λ_{em} = 500-540 nm; Red fluorescence channel: λ_{ex} = 543 nm, λ_{em} = 560-620 nm.

Mouse breast cancer 4T1 xenografted tumor-bearing BALB/c mice model

All animal procedures were performed in accordance with the Guidelines for Care and Use of Laboratory Animals of Soochow University and approved by the Animal Ethics Committee of Soochow University. The BALB/c nude mice (5-7 weeks, female) were raised at 25 °C and 55-60% humidity atmosphere. Briefly, 4T1 cells (~2×10^6) were injected subcutaneously into the forelimb of the mice to establish the solid tumor model. About 6 days later, the tumors growed to ~80 mm^3, then these tumor-bearing mice were used to follow experiments, and the tumoral hypoxia was also

confirmed by immunofluorescence imaging of HIF-1α according to reported methods.[4]

***In vivo* antitumor evaluation**

For *in vivo* hypoxic tumor growth inhibition study (intratumoral administration), the tumor-bearing mice were randomly divided into four groups (n = 5) and exposed to different treatments: group I, only administration with PBS (100 μL); group II, administration with PBS (100 μL), 0.5 h later, the tumor site was irradiated with white LED lamp (100 mW cm^{-2}, 30 min); group III, administration with ^{mito}ZnPor (1 mg mL^{-1},100 μL); group IV, administration with ^{mito}ZnPor (1 mg mL^{-1},100 μL), 0.5 h later, the tumor site was irradiated with white LED lamp (100 mW cm^{-2}, 30 min). On day 4, all above mentioned treatments were repeated one more time. During the whole therapeutic course (14 d), the tumor volume of all mice was measured every other day, and the volumn calculation formula was as follows: V = width × width × length/2. On day 5 post-treatment, one tumor in each group was collected and stained by H&E and TUNEL staining for histological analysis.

***In vivo* biosafety assay**

On day 14, all mice were euthanized, and the blood of mice was collected for a routine blood test and blood biochemical test. And all normal organs including heart, liver, spleen, lung, and kidney were also collected for histological analysis via H&E staining to evaluate biosafety.

Statistical analysis

Data were expressed as mean ± standard deviation. Two-tailed Student's t-test was used to evaluate the statistical significance. P values < 0.05 were regarded to be statistically significant (*p < 0.05, **p < 0.01, ***p < 0.001, ****p < 0.0001).

Supplementary table

Table S1 The absorption peaks of phlorins.[a]

Phl	Phl-1	Phl-2	Phl-3	Phl-4
λ_{abs} (nm)	499, 679	494, 668	501, 680	506, 689

[a] The phlorin (Phl) was obtained via NADH and cPor in deoxygenized PBS upon LED light irradiation (λ 405 nm, 25 mW cm^{-2}).

Supplementary figures

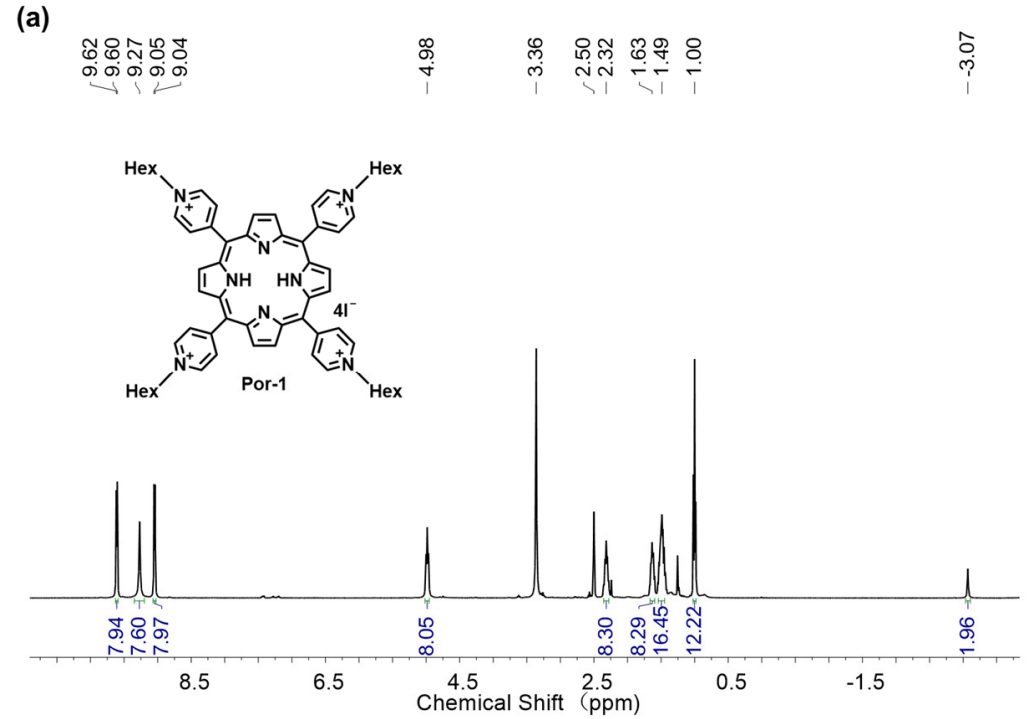

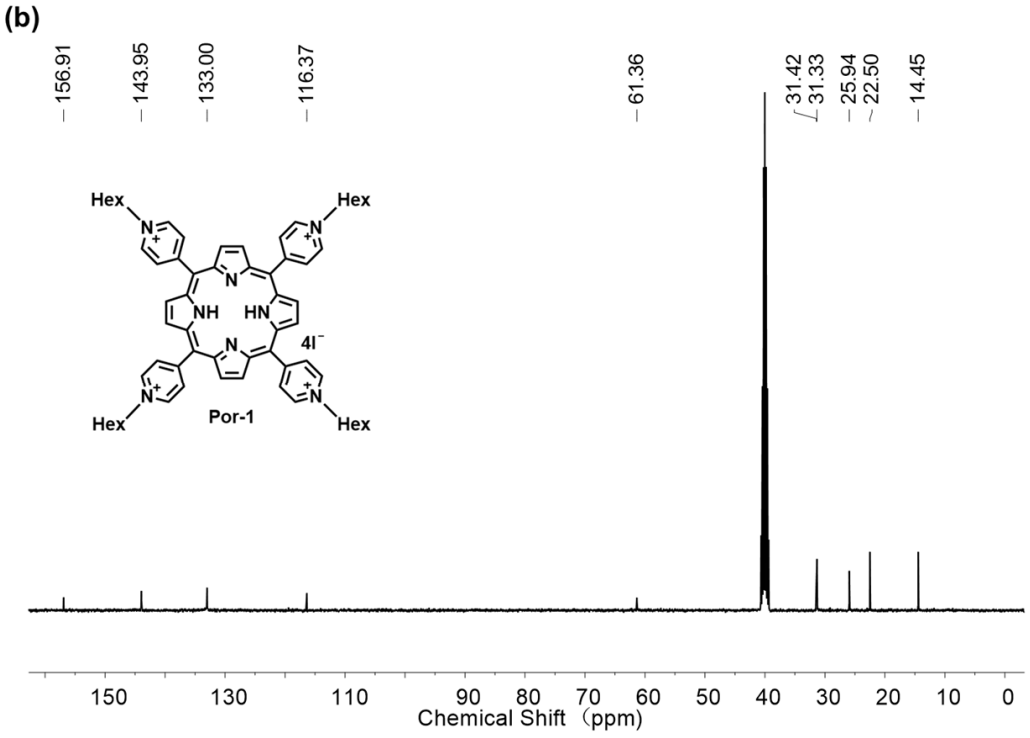

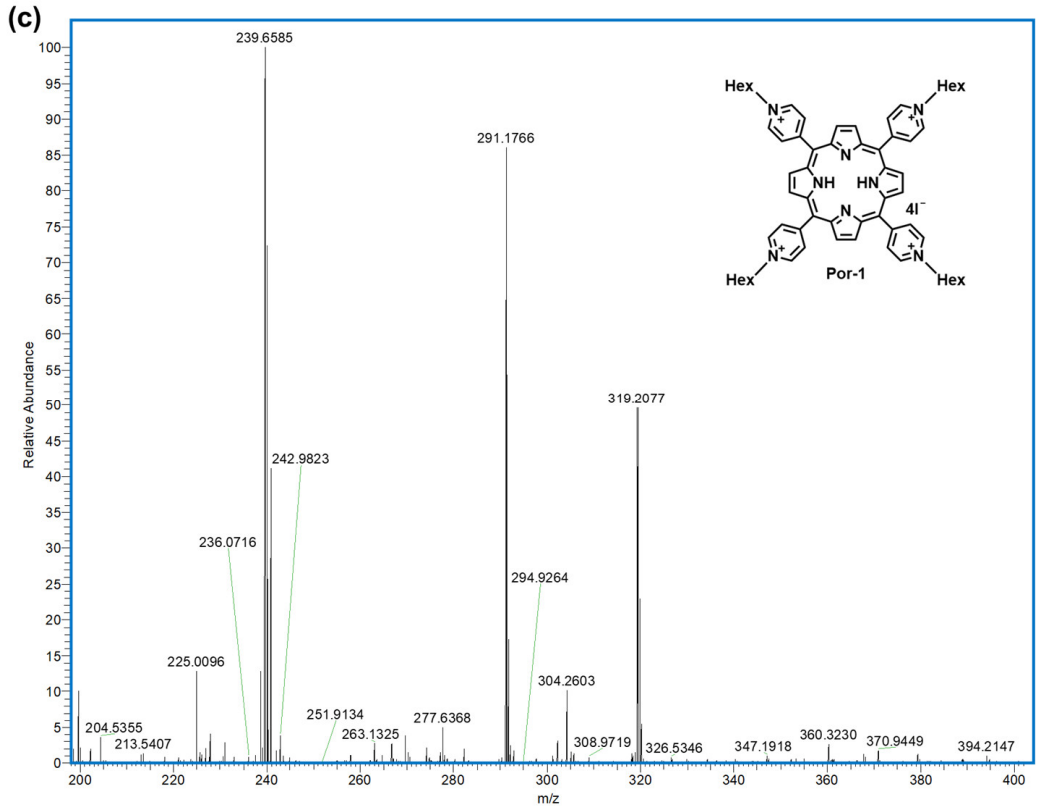

Fig. S1 (a) ^{1}H NMR and (b) ^{13}C NMR spectra of Por-1 in DMSO-d_6. (c) HRMS spectrum of Por-1.

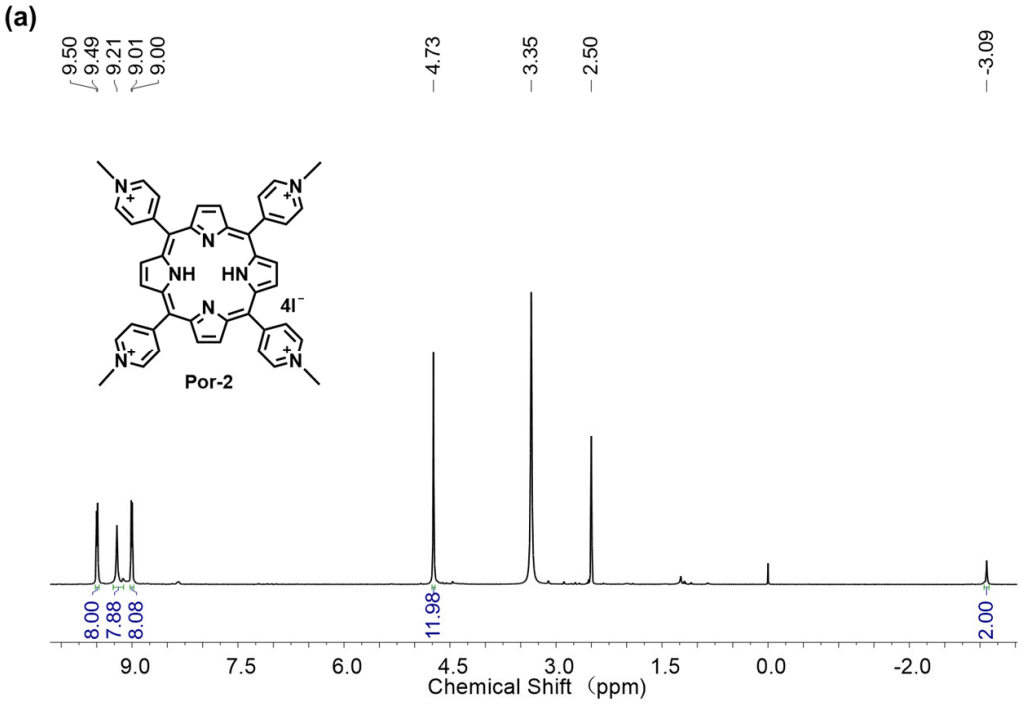

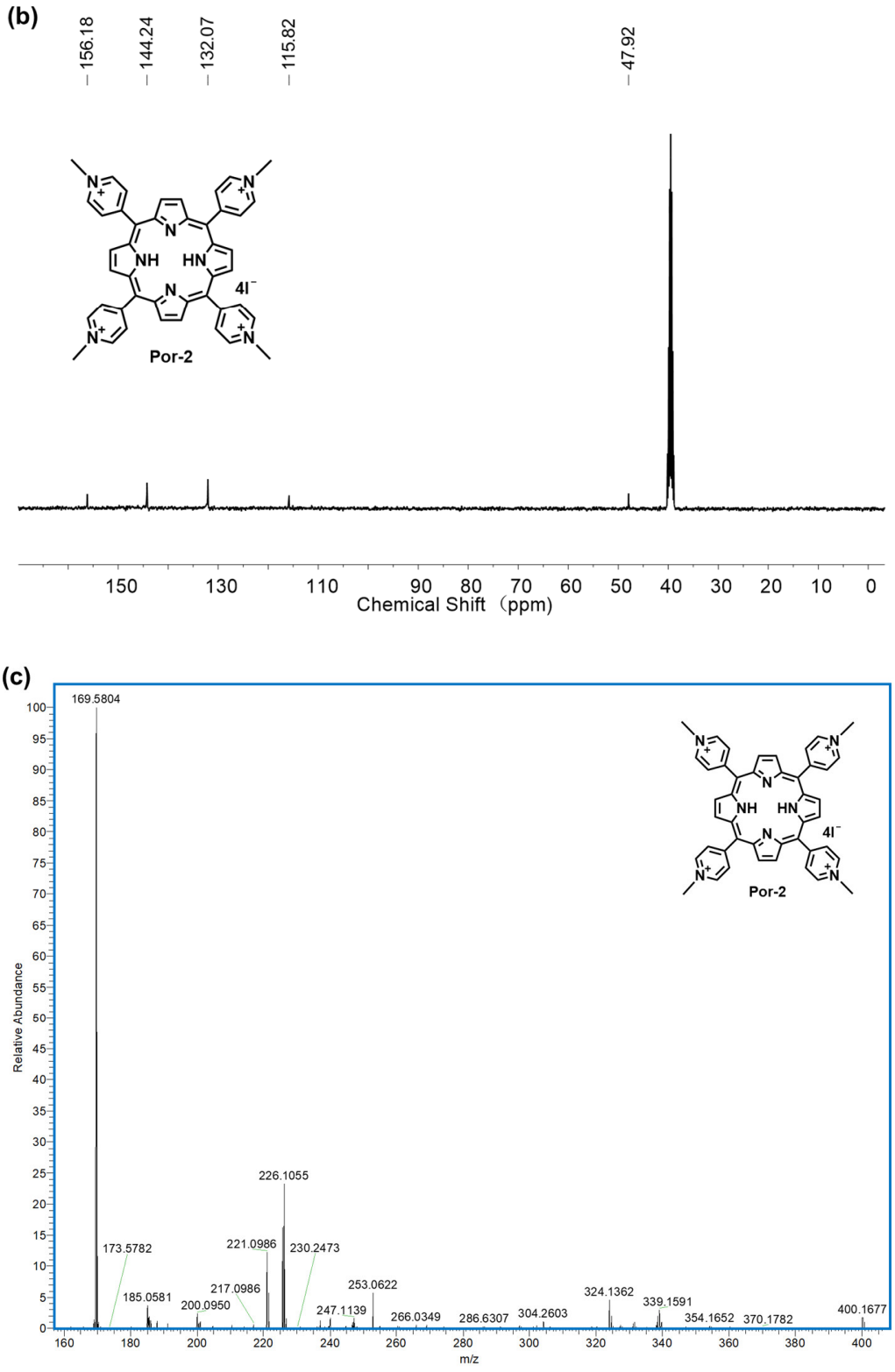

Fig. S2 (a) ^{1}H NMR and (b) ^{13}C NMR spectra of Por-2 in DMSO-d_6. (c) HRMS spectrum of Por-2.

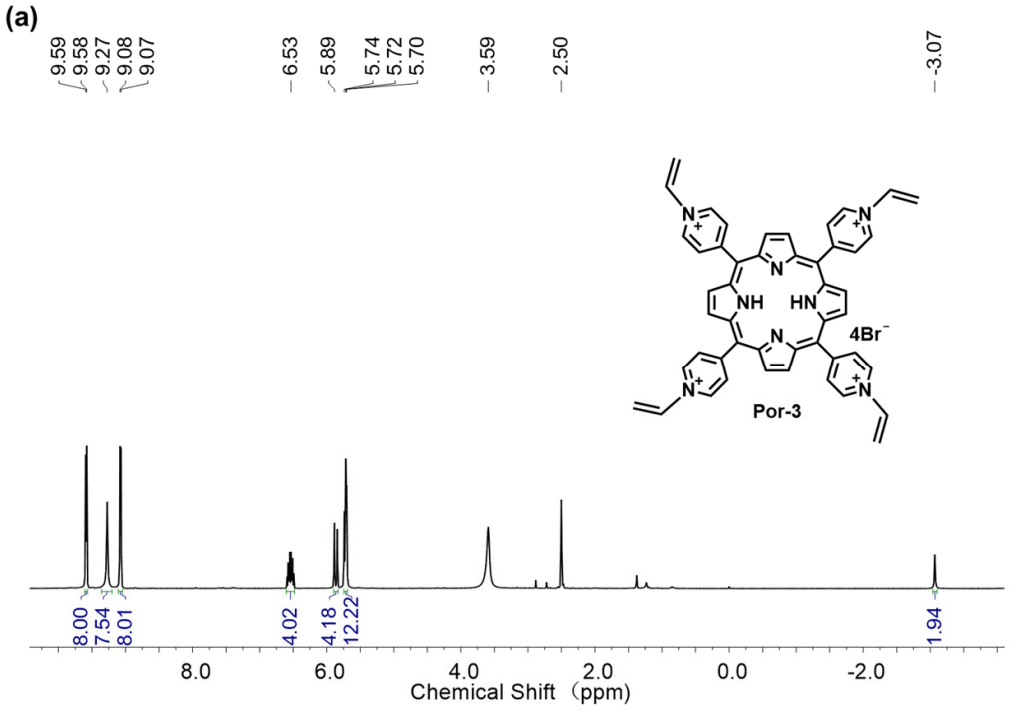
(a)
9.59
9.58
9.27
9.08
9.07
6.53
5.89
5.74
5.72
5.70
3.59
2.50
-3.07
4Br⁻
Por-3
8.00
7.54
8.01
4.02
4.18
12.22
1.94
8.0
6.0
4.0
2.0
0.0
-2.0
Chemical Shift (ppm)

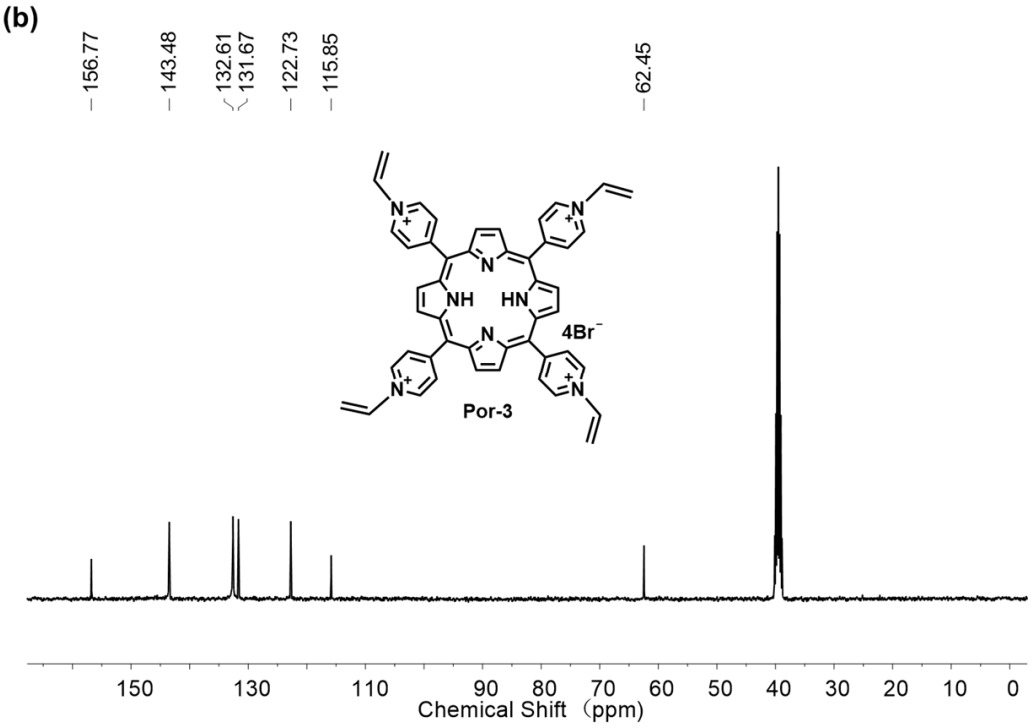
(b)
156.77
143.48
132.61
131.67
122.73
115.85
62.45
4Br⁻
Por-3
150
130
110
90
80
70
60
50
40
30
20
10
0
Chemical Shift (ppm)

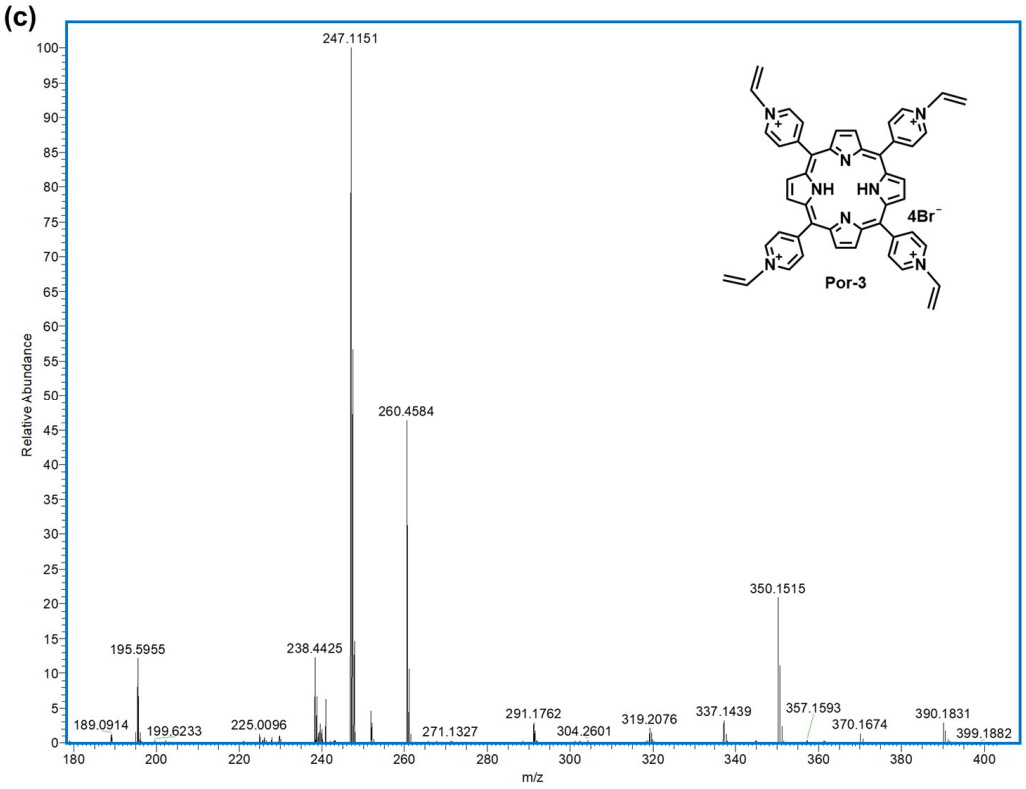

Fig. S3 (a) ^{1}H NMR and (b) ^{13}C NMR spectra of Por-3 in DMSO-d_6. (c) HRMS spectrum of Por-3.

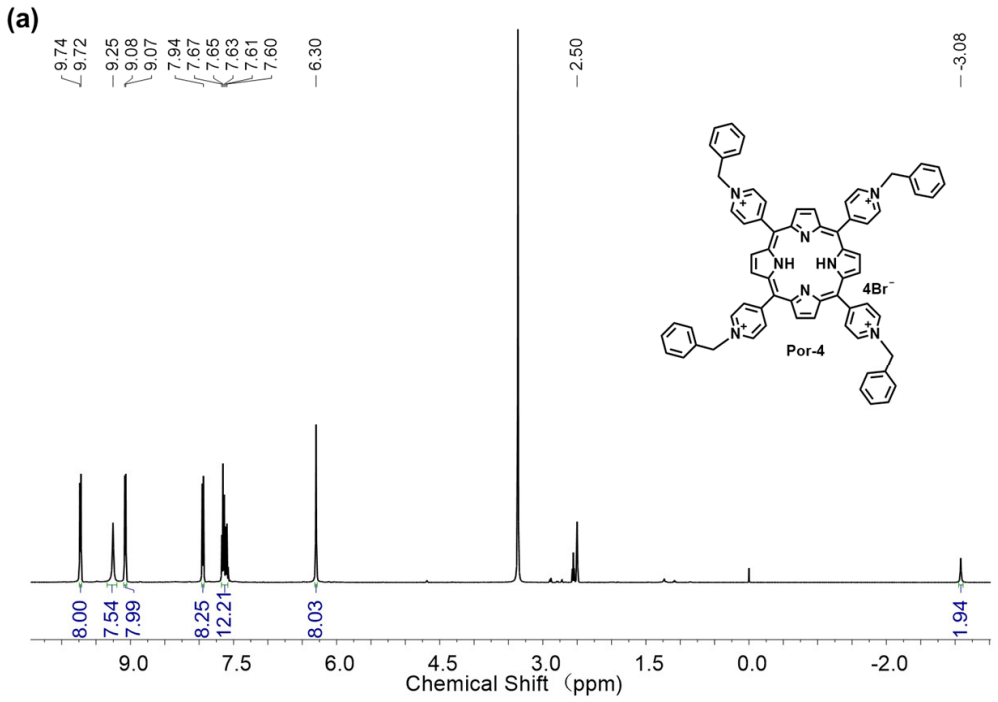

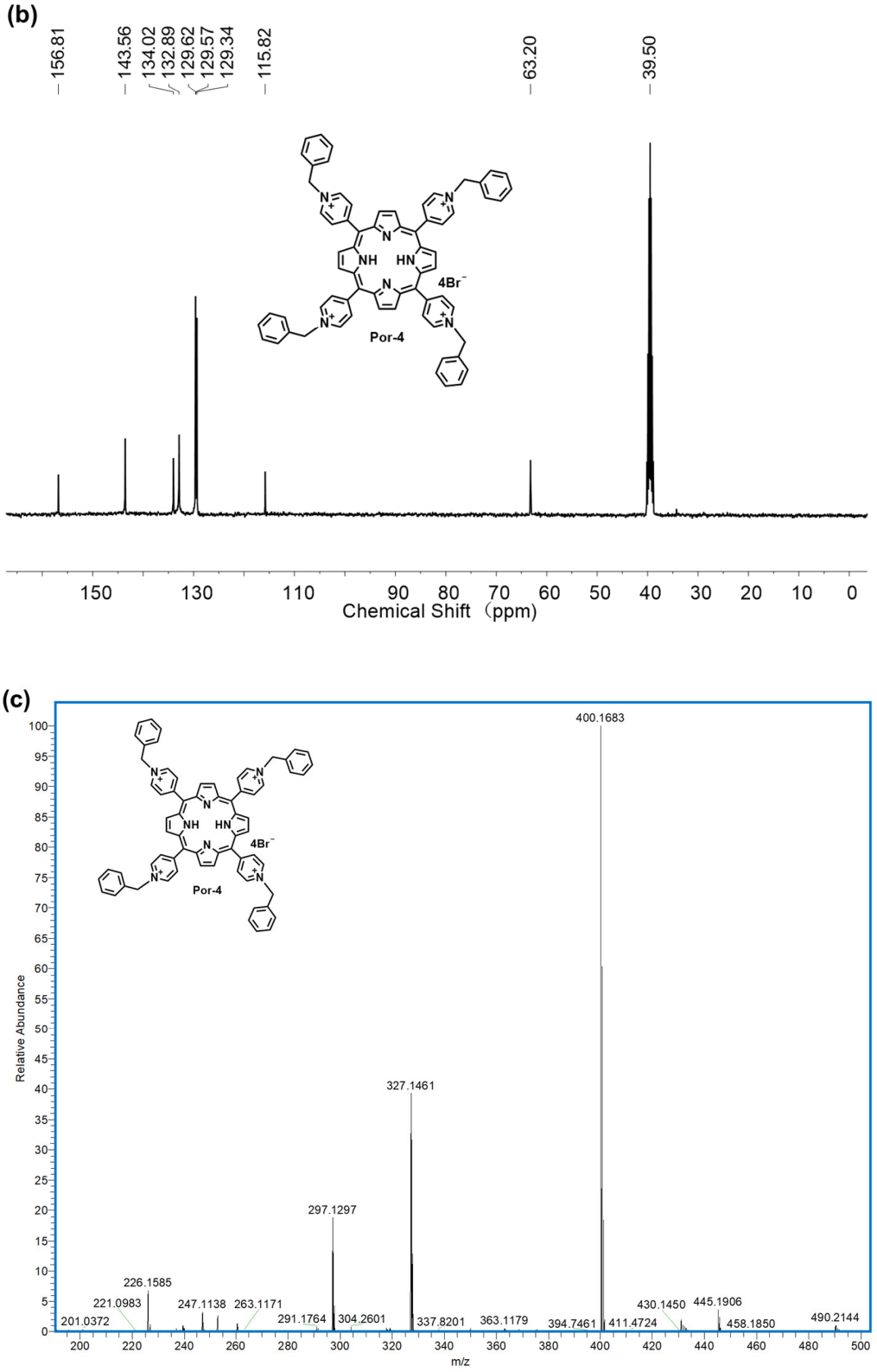

Fig. S4 (a) ^{1}H NMR and (b) ^{13}C NMR spectra of Por-4 in DMSO-d_6. (c) HRMS spectrum of Por-4.

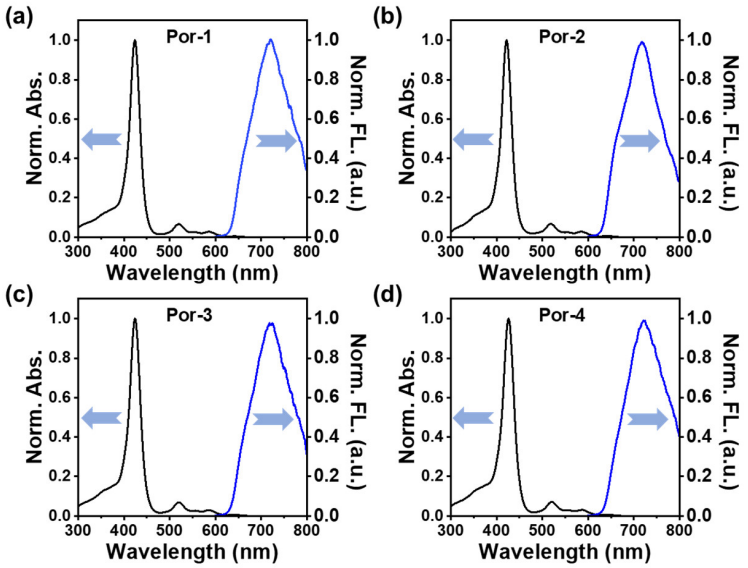

Fig. S5 Normalized UV-vis absorption (Black line) and fluorescence emission spectra (Blue line) of (a) Por-1, (b) Por-2, (c) Por-3, (d) Por-4 in pH 7.4 PBS.

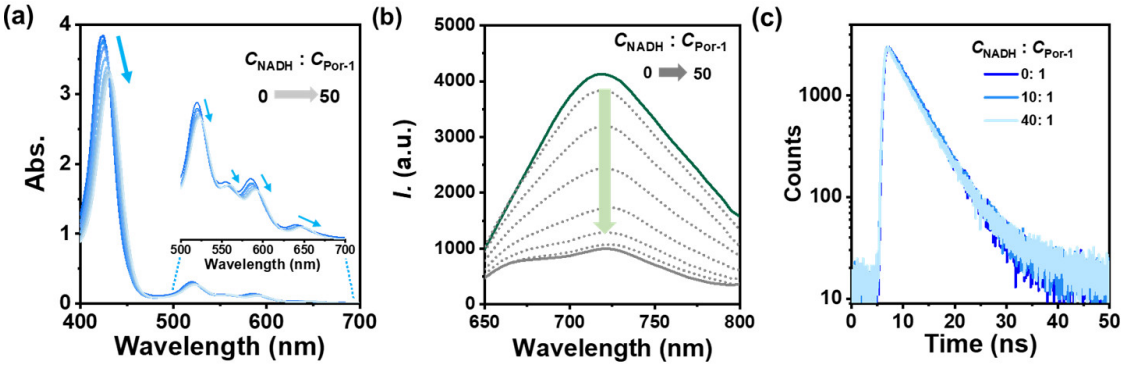

Fig. S6 (a) UV-vis absorption spectra of Por-1 (20 μM) in the presence of NADH (0~1 mM) in pH 7.4 PBS. (b) Fluorescence emission spectra of Por-1 (10 μM) in the presence of varied concentrations of NADH in PBS. (c) Fluorescence lifetime decays of Por-1 (λ_{em} = 720 nm) in PBS in the presence and absence of NADH.

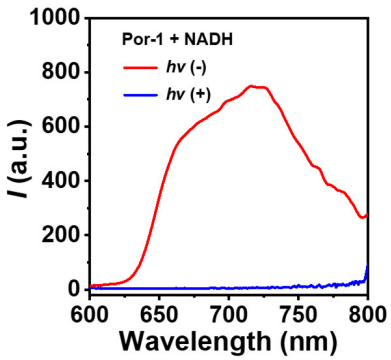

Fig. S7 The fluorescence emission spectra of solutions containing Por-1 (10 μM) and NADH (200 μM) in deoxygenized pH 7.4 PBS before and after irradiation (λ 405 nm, 25 mW cm^{-2}).

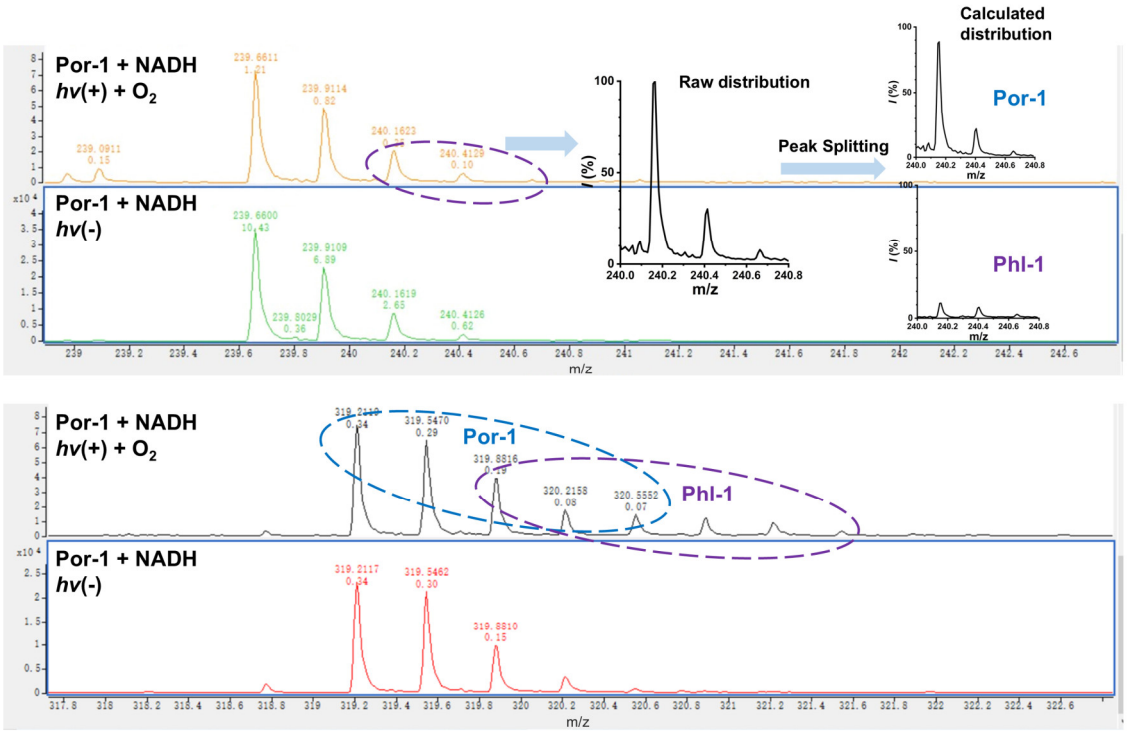

Fig. S8 HRMS spectra during the oxidation process of Phl-1.

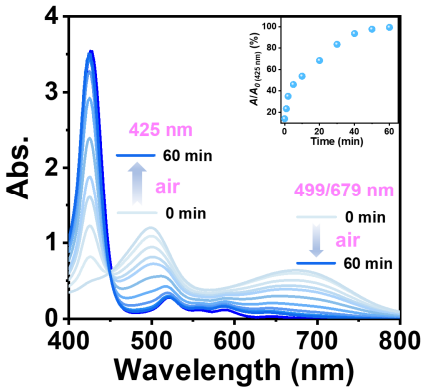

Fig. S9 UV-vis spectra of Por-1 (20 μM) and NADH (200 μM) pre and post irradiation, and exposure to air for 60 min after irradiation. Inset: the plot of A/A_0 versus time, where A_0 denoted absorption intensity of original Por-1 at 425 nm, A denoted absorption intensity at 425 nm after exposing Phl-1 to air.

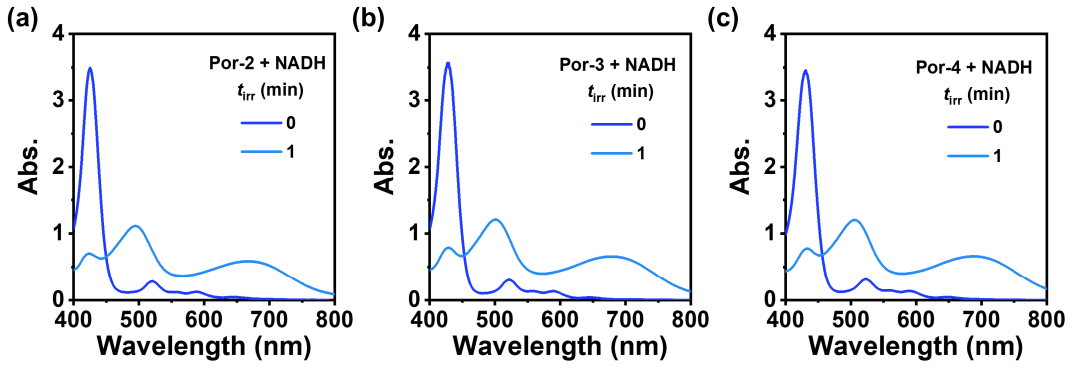

Fig. S10 UV-vis spectra of NADH (200 μM) and (a) Por-2 (20 μM), (b) Por-3 (20 μM), (c) Por-4 (20 μM) in deoxygenized PBS pre and post LED light irradiation (λ 405 nm, 25 mW cm^{-2}, 1 min).

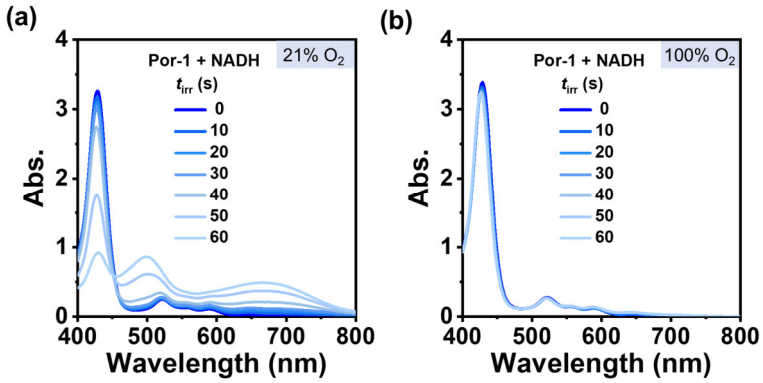

Fig. S11 Time-dependent UV-vis spectra of NADH (400 μM) and Por-1 (20 μM) in pH 7.4 PBS upon LED light irradiation (λ 405 nm, 25 mW cm^{-2}). (a) under normoxia (21% O_2), (b) under severe hyperoxia (100% O_2).

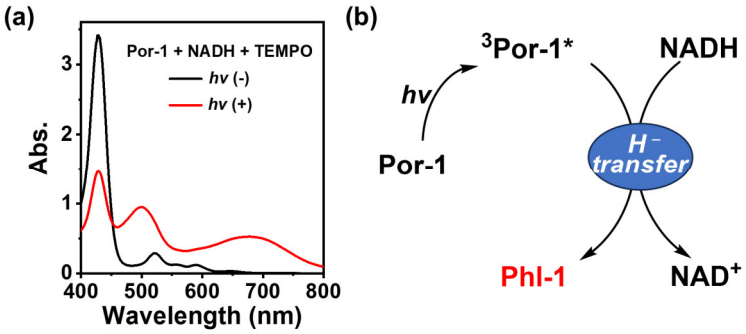

Fig. S12 (a) UV-vis spectra of Por-1 (20 μM), NADH (200 μM) and TEMPO (10 mM) in deoxygenized PBS pre and post light irradiation (λ 405 nm, 25 mW cm^{-2}). (b) Proposed reaction mechanism of Por-1 with NADH under hypoxia.

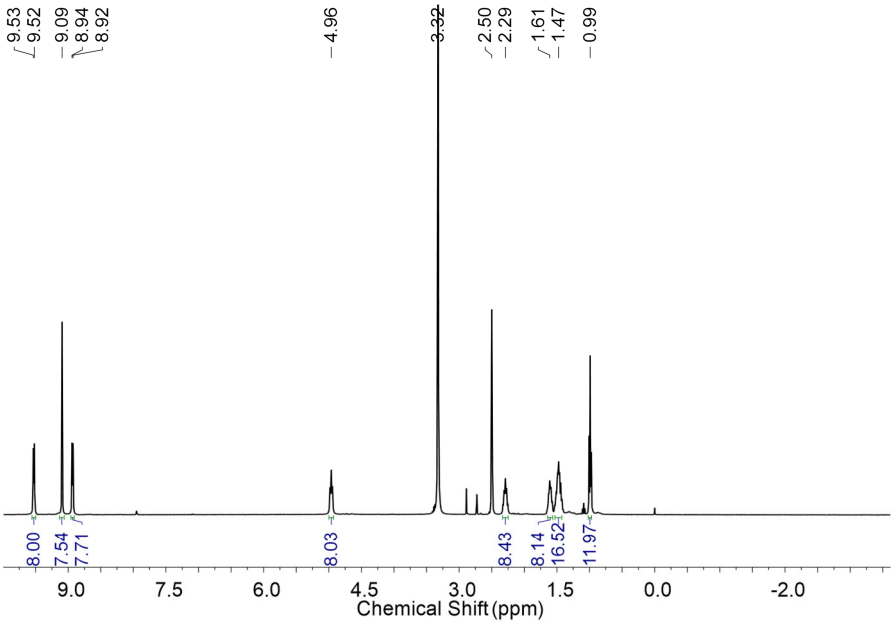

Fig. S13 ^{1}H NMR spectrum of ZnPor in DMSO-d_6 (400 MHz).

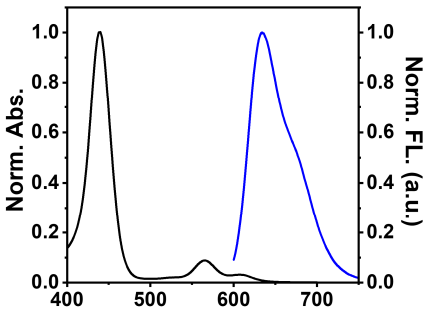

Fig. S14 Normalized UV-vis absorption (Black line) and fluorescence emission spectra (Blue line) of ZnPor.

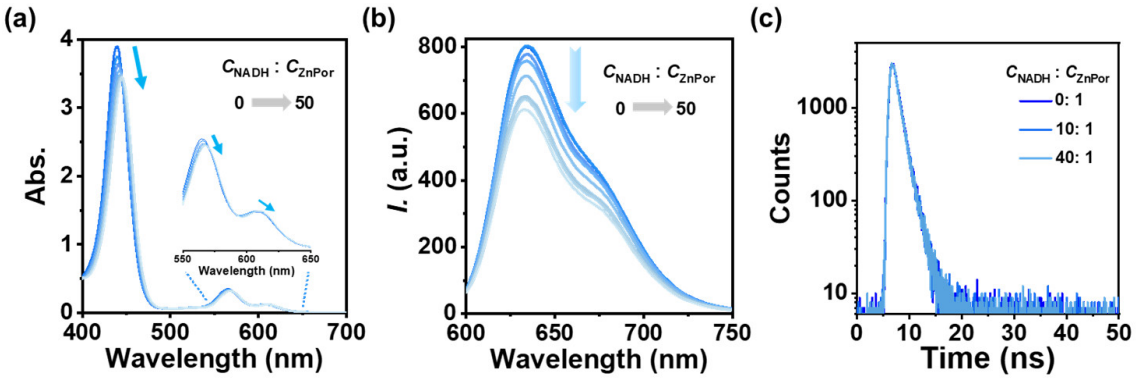

Fig. S15 (a) UV-vis absorption spectra of ZnPor (20 μM) in the presence of NADH (0~1 mM) in pH 7.4 PBS. (b) Fluorescence emission spectra of ZnPor (10 μM) in the presence of NADH (0~500 μM) in pH 7.4 PBS. (c) Fluorescence lifetime decays of ZnPor (λ_{em} = 640 nm) in pH 7.4 PBS in the presence and absence of NADH.

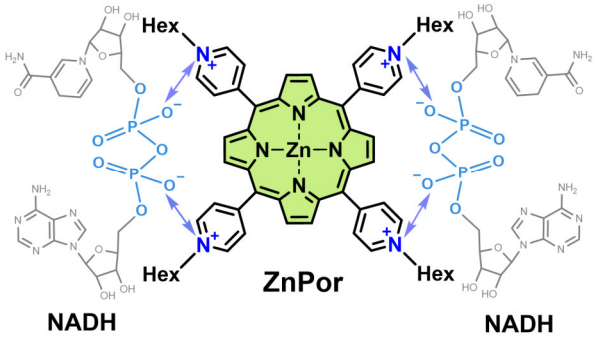

Fig. S16 Schematic illustration of electrostatic interactions between ZnPor and NADH.

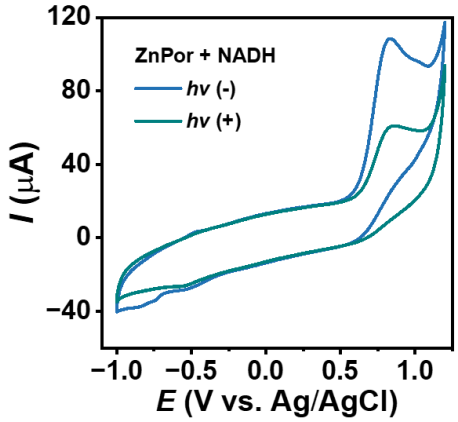

Fig. S17 Cyclic voltammograms of ZnPor/NADH system pre and post irradiation.

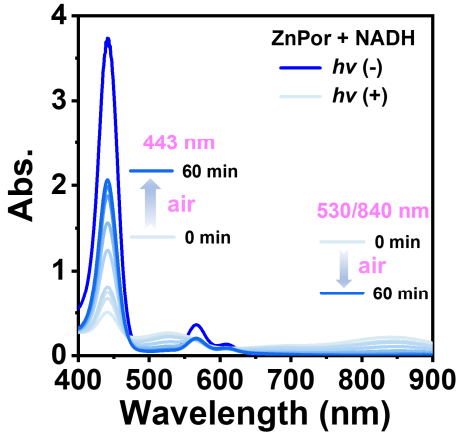

Fig. S18 UV-vis spectra of ZnPor (20 μM) and NADH (200 μM) before and after irradiation, and exposure to air for 60 min after irradiation.

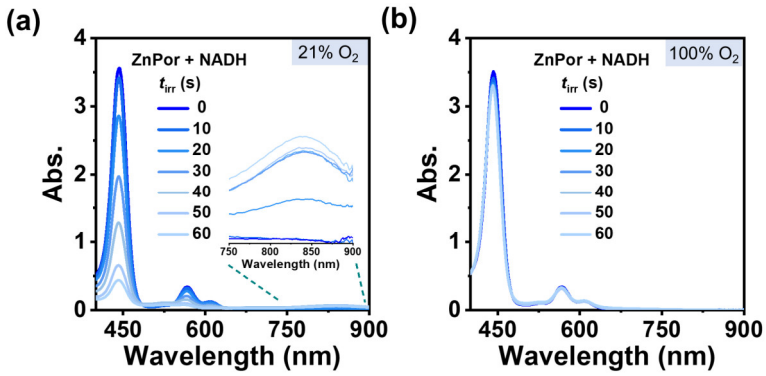

Fig. S19 Time-dependent UV-vis spectra of NADH (400 μM) and ZnPor (20 μM) in pH 7.4 PBS upon LED light irradiation (λ 405 nm, 25 mW cm^{-2}). (a) under normoxia (21% O_2), (b) under severe hyperoxia (100% O_2).

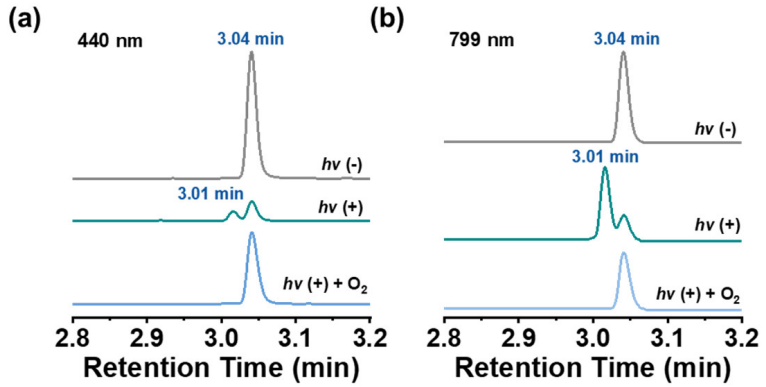

Fig. S20 UPLC analysis of the solution containing ZnPor (20 μM) and NADH (200 μM) in deoxygenated pH 7.4 PBS pre and post light irradiation (λ 405 nm, 25 mW cm^{-2}, t_{irr} = 5 s), and exposure to oxygen after irradiation. (a) 440 nm channel, (b) 799 nm channel.

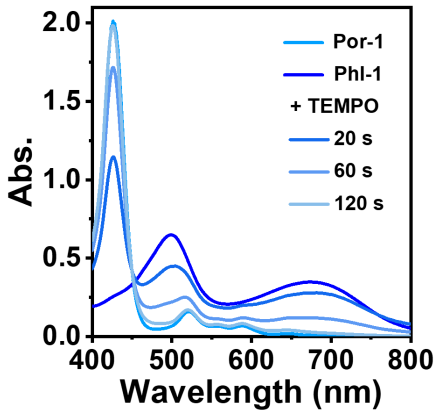

Fig. S21 UV-vis spectra of solution containing Phl-1 pre and post addition of TEMPO (10 mM).

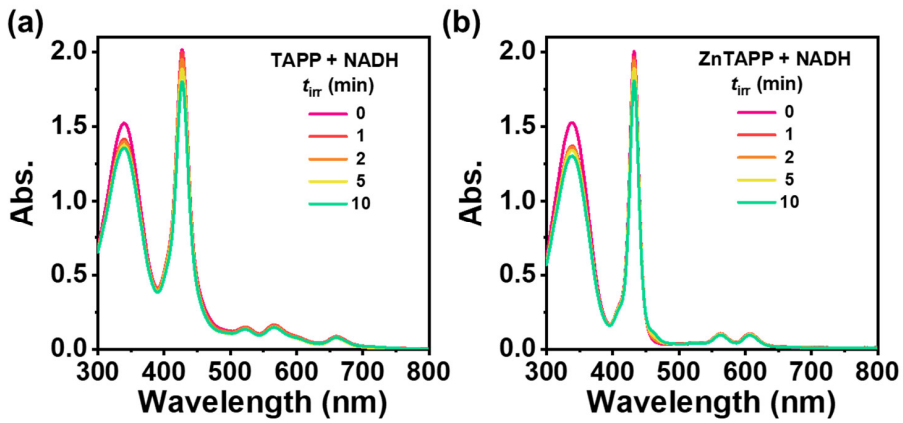

Fig. S22 (a) Time-dependent UV-vis spectra of TAPP (20 μM) and NADH (200 μM) in deoxygenized 30% THF/PBS upon LED light irradiation (λ 405 nm, 25 mW cm^{-2}). (b) Time-dependent UV-vis spectra of ZnTAPP (20 μM) and NADH (200 μM) in deoxygenized 30% THF/PBS upon LED light irradiation (λ 405 nm, 25 mW cm^{-2}).

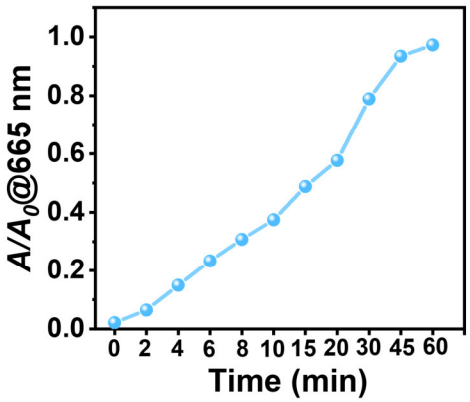

Fig. S23 The change of A/A_0 (665 nm) after the irradiated solution containing ZnPor (1 μM), NADH (100 μM) and MB (10 μM) was exposed to air for various periods (0~60 min).

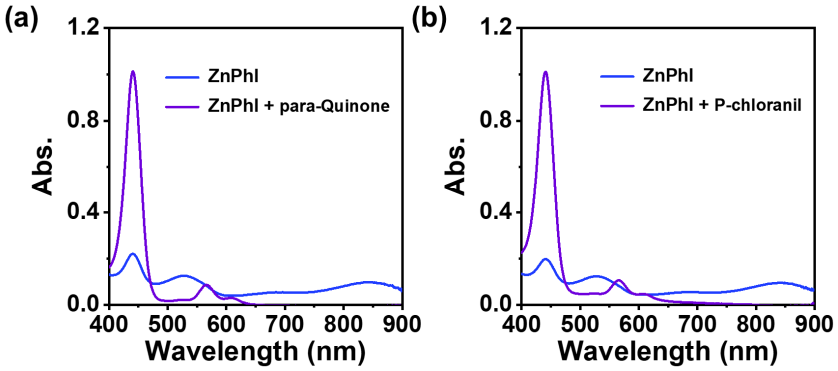

Fig. S24 UV-vis spectra of solutions containing ZnPhl pre and post adding (a) para-quinone and (b) p-chloranil.

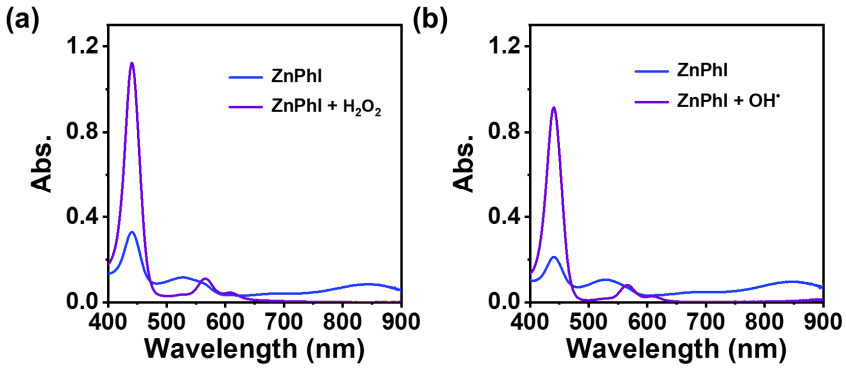

Fig. S25 UV-vis spectra of solutions containing ZnPhl pre and post adding (a) H_2O_2 and (b) OH•.

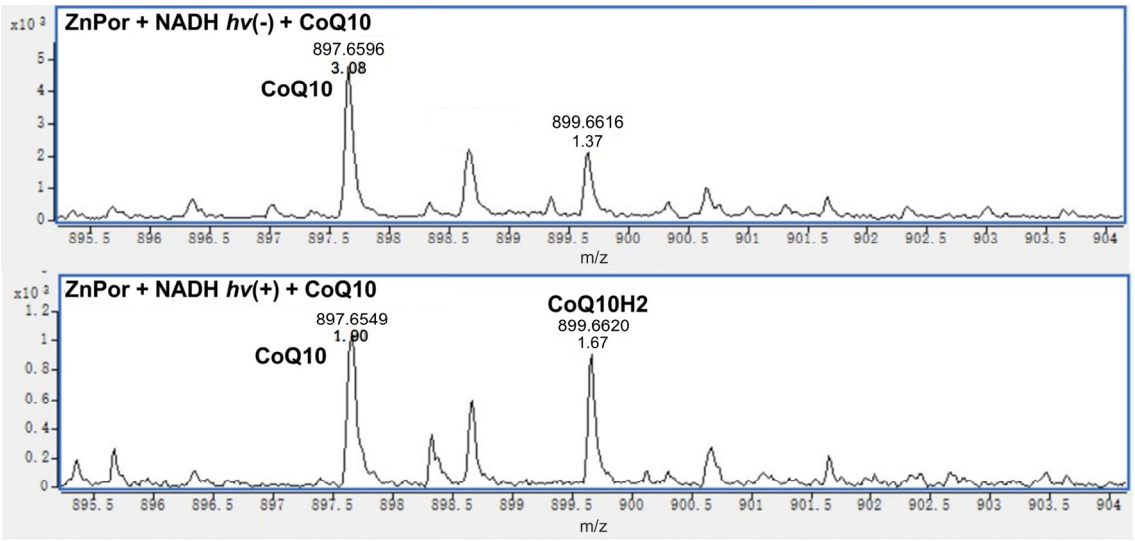

Fig. S26 HRMS spectra after adding CoQ10 to ZnPor (top) or ZnPhl (bottom).

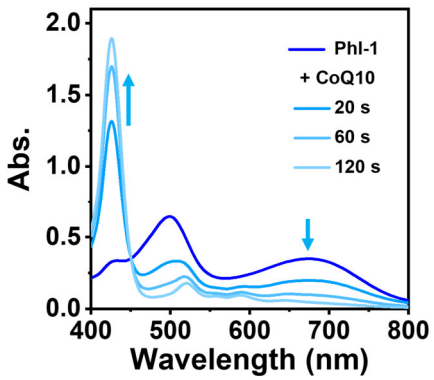

Fig. S27 UV-vis spectra of solutions containing Phl-1 before and after adding CoQ10.

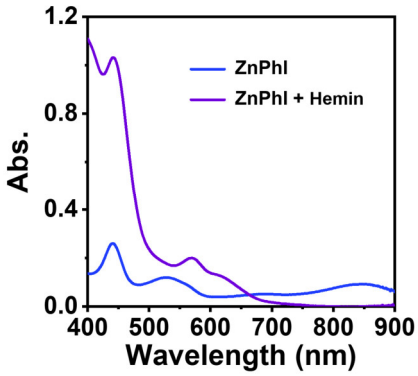

Fig. S28 UV-vis spectra of solutions containing ZnPhl before and after adding hemin.

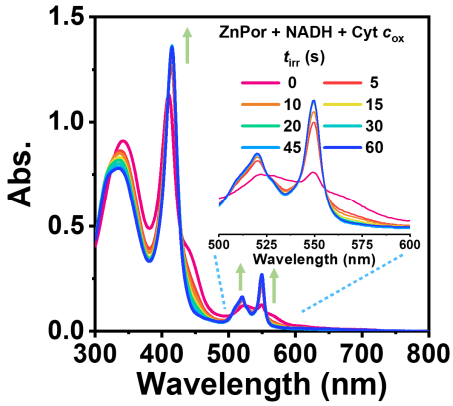

Fig. S29 UV-vis spectra of solutions containing ZnPor (1 μM), NADH (100 μM) and Cyt c_{ox} (0.1 mg mL^{-1}) before and after LED light irradiation (λ 405 nm, 25 mW cm^{-2}).

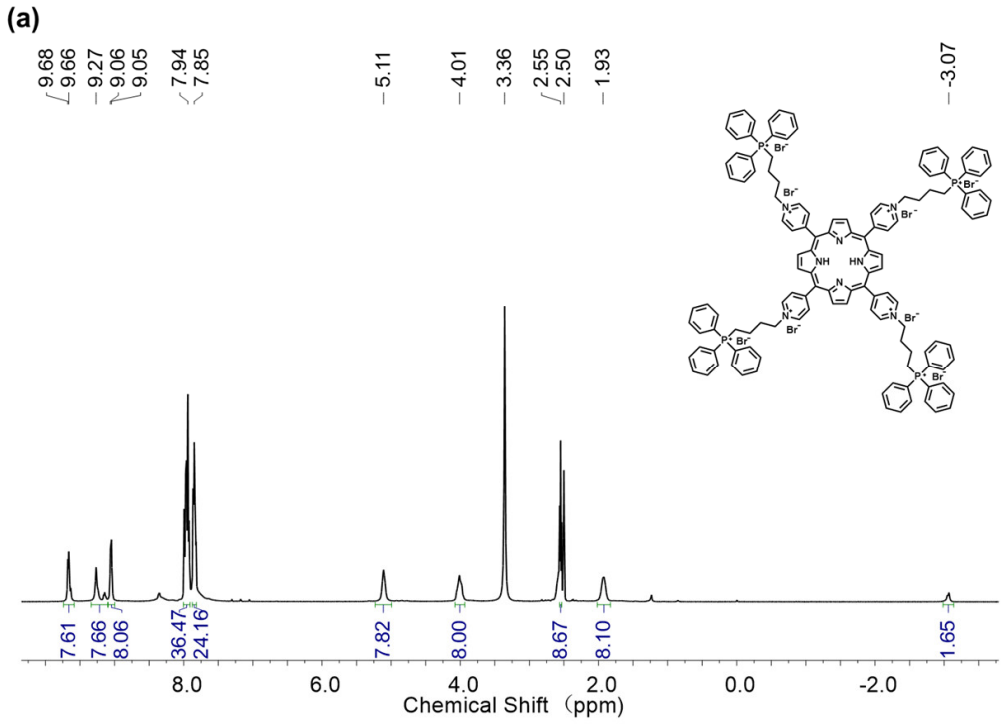

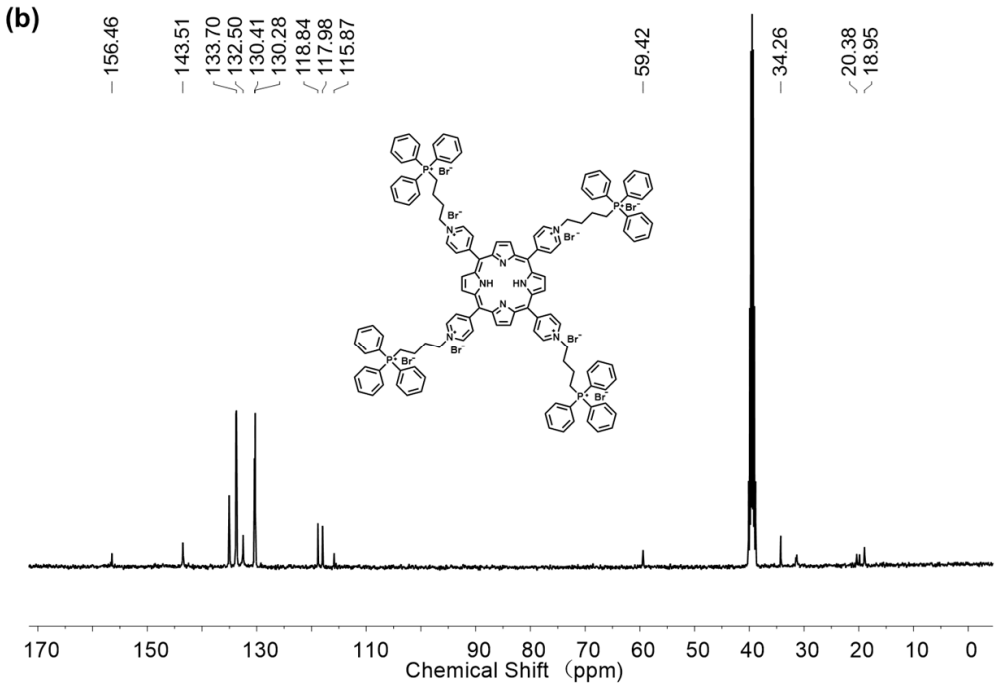
(b)
156.46
143.51
133.70
132.50
130.41
130.28
118.84
117.98
115.87
59.42
34.26
20.38
18.95
170
150
130
110
90
80
70
60
50
40
30
20
10
0
Chemical Shift (ppm)

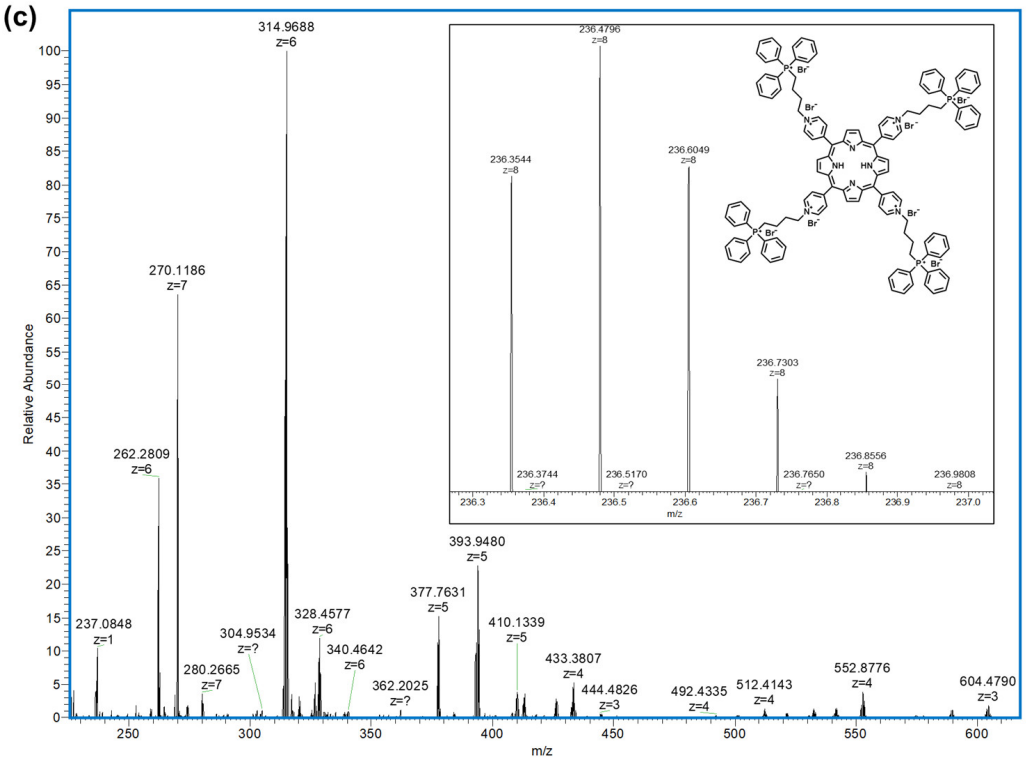
(c)
Relative Abundance
m/z
314.9688
z=6
270.1186
z=7
262.2809
z=6
237.0848
z=1
280.2665
z=7
304.9534
z=?
328.4577
z=6
340.4642
z=6
362.2025
z=?
377.7631
z=5
393.9480
z=5
410.1339
z=5
433.3807
z=4
444.4826
z=3
492.4335
z=4
512.4143
z=4
552.8776
z=4
604.4790
z=3
236.4796
z=8
236.3544
z=8
236.6049
z=8
236.7303
z=8
236.3744
z=?
236.5170
z=?
236.7650
z=?
236.8556
z=8
236.9808
z=8

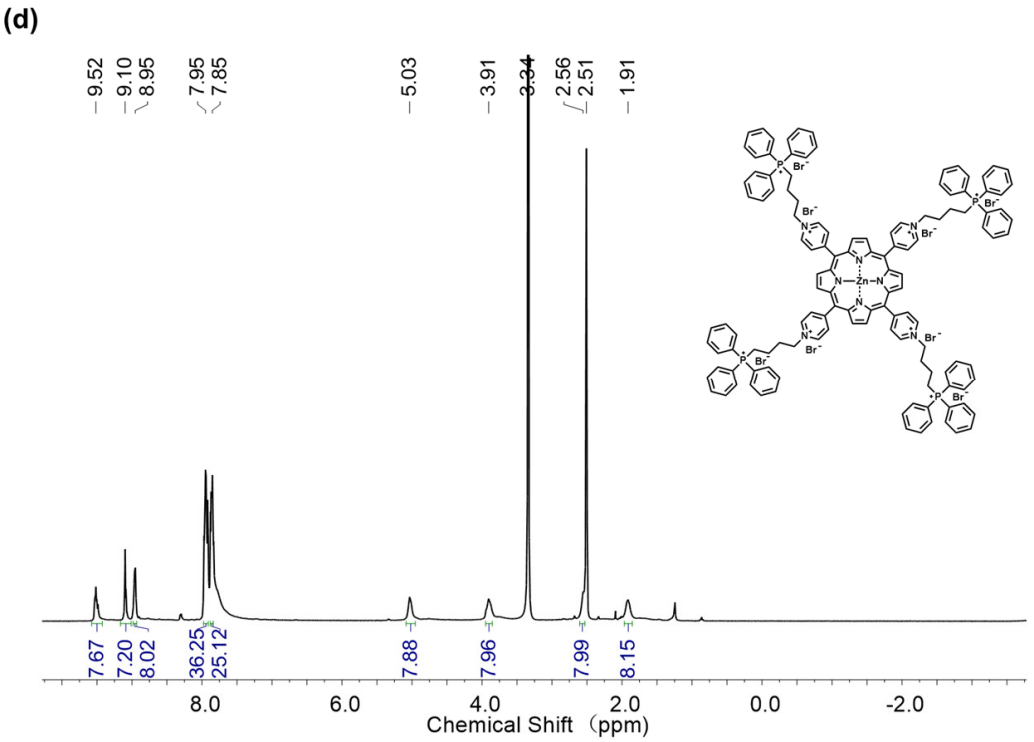

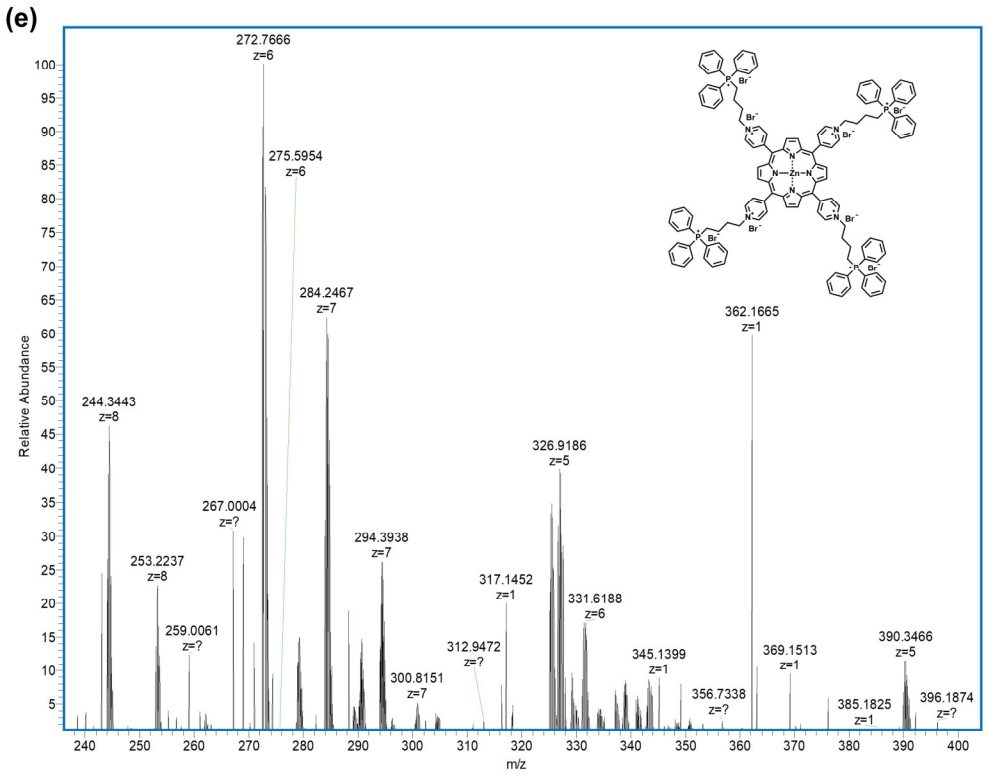

Fig. S30 (a) ^{1}H NMR and (b) ^{13}C NMR spectra of ^{mito}Por in DMSO-d_6. (c) HRMS spectrum of ^{mito}Por. (d) ^{1}H NMR spectra of ^{mito}ZnPor in DMSO-d_6. (e) HRMS spectrum of ^{mito}ZnPor.

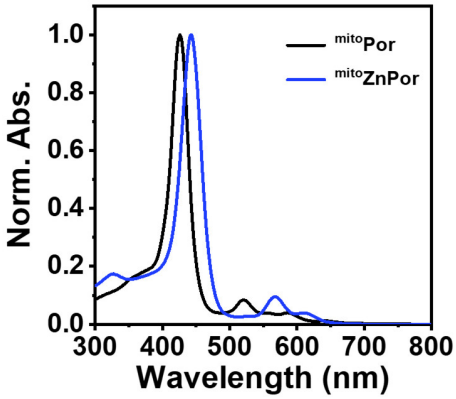

Fig. S31 Normalized UV-vis spectra of ^{mito}Por and ^{mito}ZnPor.

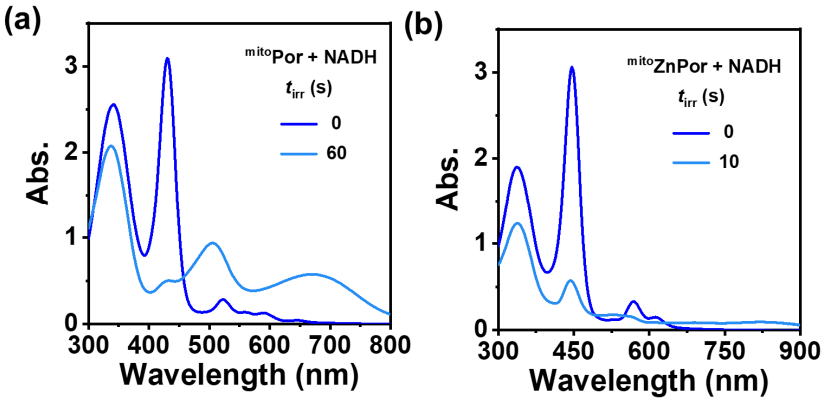

Fig. S32 (a) UV-vis spectra of ^{mito}Por (15 μM) and NADH (400 μM) in deoxygenized PBS pre and post LED light irradiation (λ 405 nm, 25 mW cm^{-2}). (b) UV-vis spectra of ^{mito}ZnPor (30 μM) and NADH (200 μM) in deoxygenized PBS pre and post LED light irradiation (λ 405 nm, 25 mW cm^{-2}).

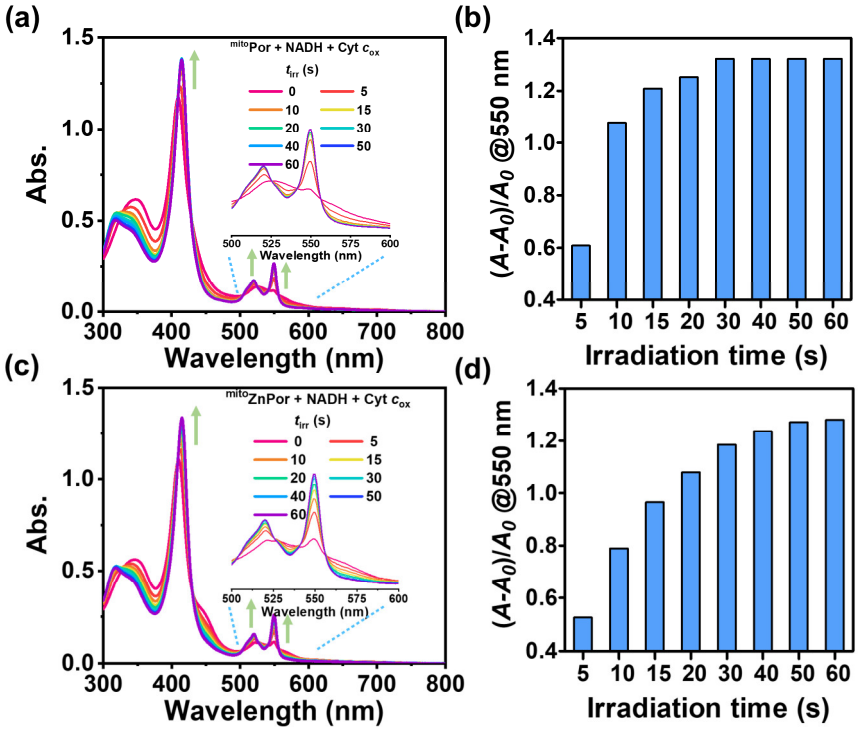

Fig. S33 (a) UV-vis spectra of solutions containing ^{mito}Por (1 μM), NADH (50 μM) and Cyt c_{ox} (0.1 mg mL^{-1}) with irradiation time (λ 405 nm, 25 mW cm^{-2}). (b) ^{mito}Por-mediated Cyt c_{ox} photoreduction efficiency in deoxygenized PBS. C (^{mito}Por) = 1 μM, C (NADH) = 50 μM, C (Cyt c_{ox}) = 0.1 mg mL^{-1}. (c) UV-vis spectra of solutions containing ^{mito}ZnPor (1 μM), NADH (50 μM) and Cyt c_{ox} (0.1 mg mL^{-1}) with irradiation time (λ 405 nm, 25 mW cm^{-2}). (d) ^{mito}ZnPor-mediated Cyt c_{ox} photoreduction efficiency in deoxygenized PBS. C (^{mito}ZnPor) = 1 μM, C (NADH) = 50 μM, C (Cyt c_{ox}) = 0.1 mg mL^{-1}.

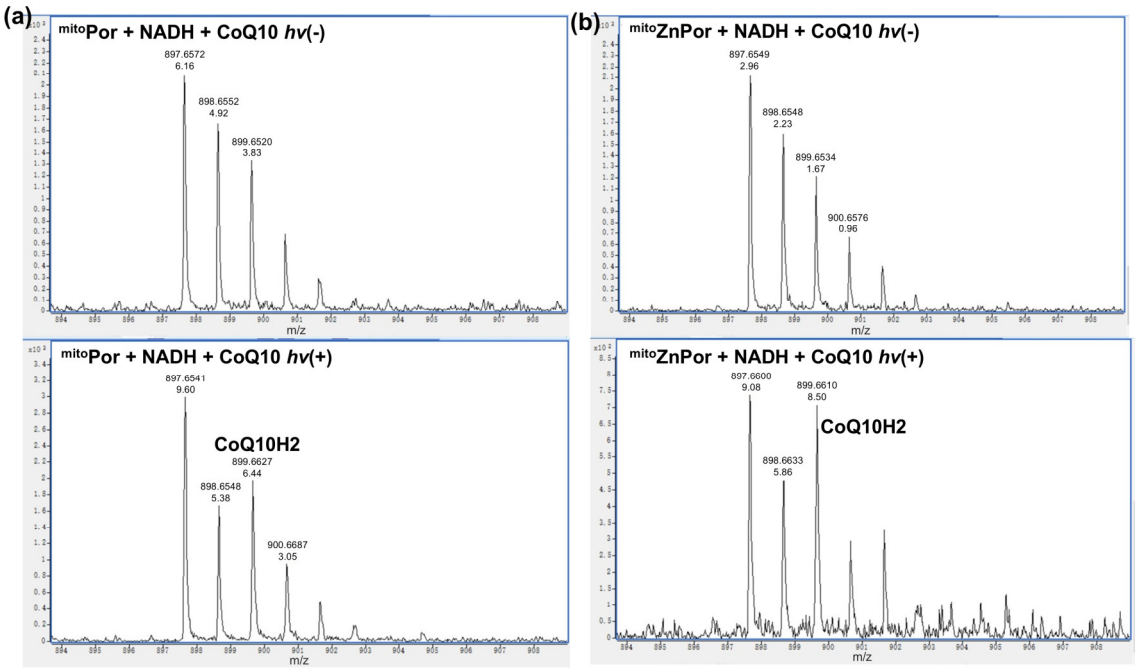

Fig. S34 (a) Top: HRMS spectrum of the mixture containing CoQ10 (5 μM), ^{mito}Por (0.1 μM) and NADH (10 μM) in the dark. Bottom: HRMS spectrum of the irradiated mixture of CoQ10 (5 μM), ^{mito}Por (0.1 μM) and NADH (10 μM). (b) Top: HRMS spectrum of the mixture containing CoQ10 (5 μM), ^{mito}ZnPor (0.2 μM) and NADH (10 μM) in the dark. Bottom: HRMS spectrum of the irradiated mixture of CoQ10 (5 μM), ^{mito}ZnPor (0.2 μM) and NADH (10 μM).

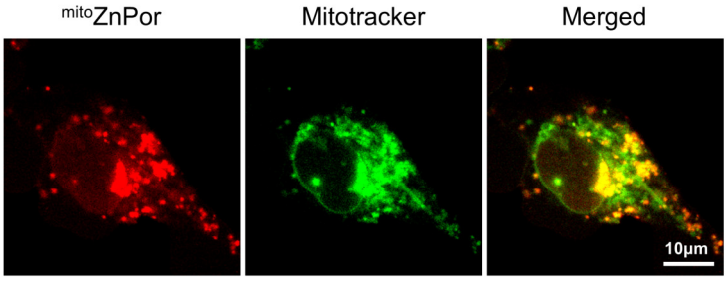

Fig. S35 CLSM images of A549 cells treated with ^{mito}ZnPor (4 μM) for 4 h in dark and then stained with Mitotracker.

Fig. S36 The photograph of mimicking hypoxic environment via Mitsubishi™ device for 4 h and measuring the content of O_2 using the oxygen indicator. Results are presented through three repeated measurements.

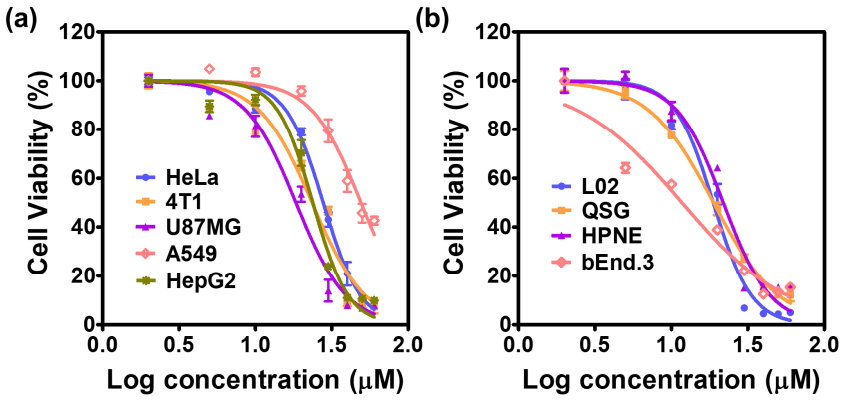

Fig. S37 (a) Viabilities of cancer cells (HeLa, 4T1, U87MG, A549, HepG2) treated with varied concentrations of ^{mito}ZnPor (0~60 μM) under hypoxia in the dark. (b) Viabilities of normal cells (L02, QSG, HPNE, bEnd.3) treated with varied concentrations of ^{mito}ZnPor (0~60 μM) under hypoxia in the dark.

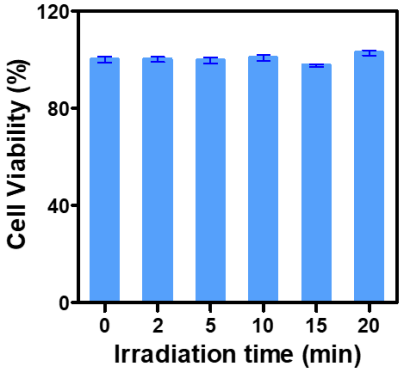

Fig. S38 Viabilities of HeLa cells irradiated with different time (0~20 min) using white LED light (30 mW cm^{-2}) under hypoxia.

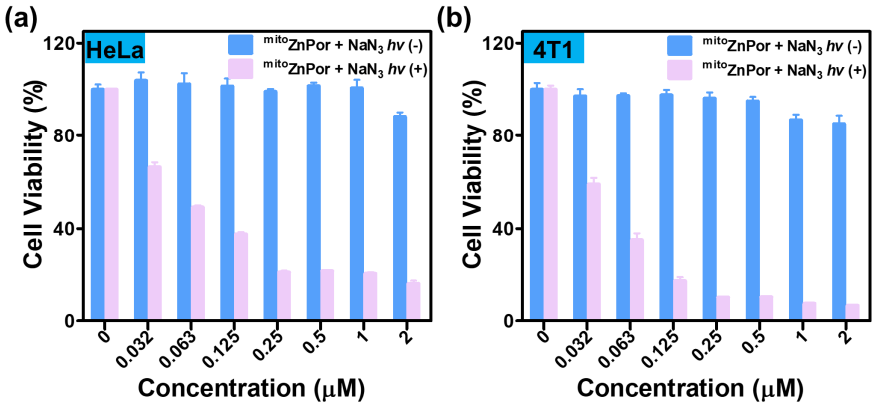

Fig. S39 Viabilities of (a) HeLa cells and (b) 4T1 cells treated with NaN_3 (10 mM) and varied concentrations of ^{mito}ZnPor (0~2 μM) in the absence and presence of white LED light irradiation (30 mW cm^{-2}, t_{irr} = 10 min) under hypoxia.

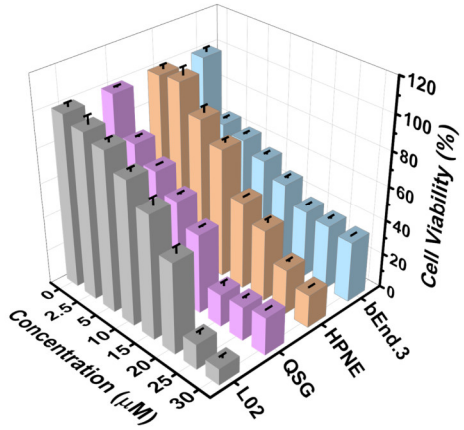

Fig. S40 Viabilities of normal cells (L02, QSG, HPNE, bEnd.3) treated with varied concentrations of ^{mito}ZnPor (0~30 μM) after white LED light irradiation (30 mW cm^{-2}, t_{irr} = 10 min) under hypoxia.

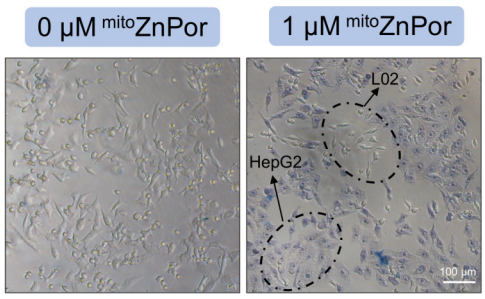

Fig. S41 The images of HepG2 and L02 cells in co-culture model treated with ^{mito}ZnPor after white LED light irradiation (30 mW cm^{-2}, t_{irr}= 10 min) under hypoxia. The cells were stained by trypan blue stain (0.4%). Scale bar, 100 μm.

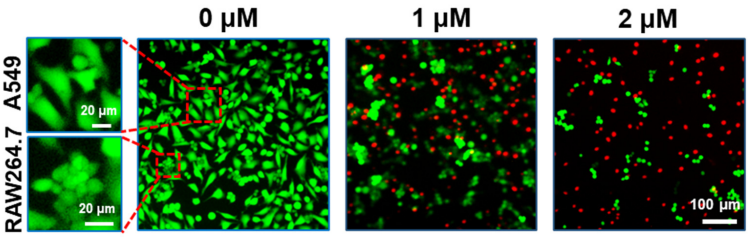

Fig. S42 The images of ^{mito}ZnPor-treated A549/RAW264.7 cells in co-cultured model after white LED light irradiation (30 mW cm^{-2} , t_{irr} = 10 min) under hypoxia. The cells were stained by Calcein-AM and PI before imaging.

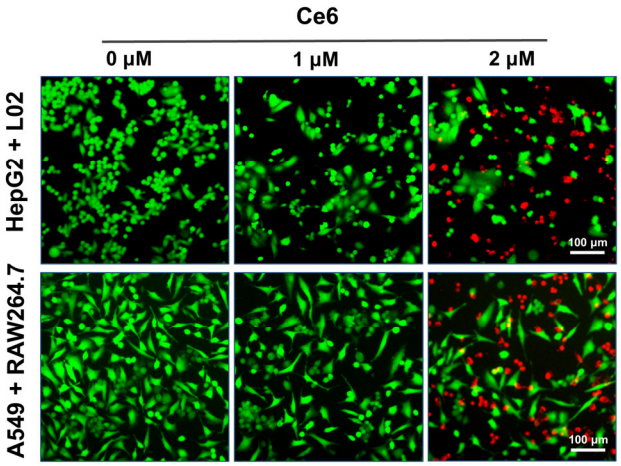

Fig. S43 Fluorescence imaging of Ce6-treated HepG2/L02 cells and A549/RAW264.7 cells in co-cultured model after white LED light irradiation (30 mW cm^{-2}, t_{irr} = 10 min) under hypoxia. The live and dead cells were stained by Calcein-AM and PI before imaging. Scale bar, 100 μm.

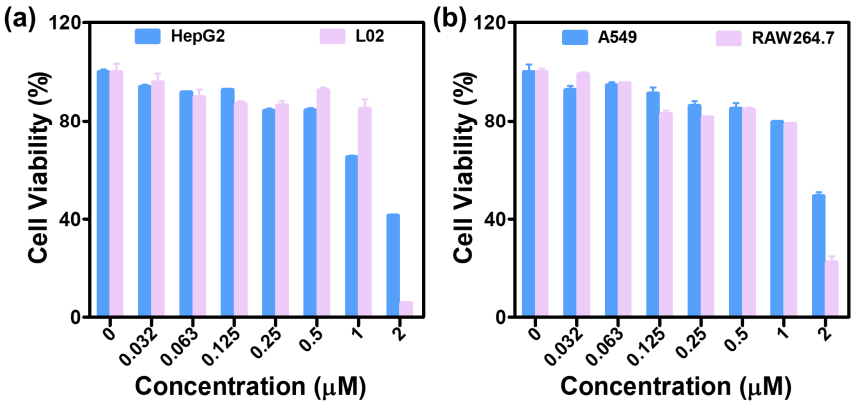

Fig. S44 (a) Viabilities of HepG2/L02 cells treated with varied concentrations of Ce6 (0~2 μM) after white LED light irradiation (30 mW cm^{-2}, t_{irr} = 10 min) under hypoxia. (b) Viabilities of A549/RAW264.7 cells treated with varied concentrations of Ce6 (0~2 μM) after white LED light irradiation (30 mW cm^{-2}, t_{irr} = 10 min) under hypoxia.

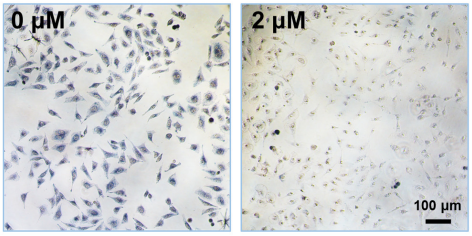

Fig. S45 Formazan formation in HeLa cells after treated with 0 or 2 μM ^{mito}ZnPor and light irradiation under hypoxia.

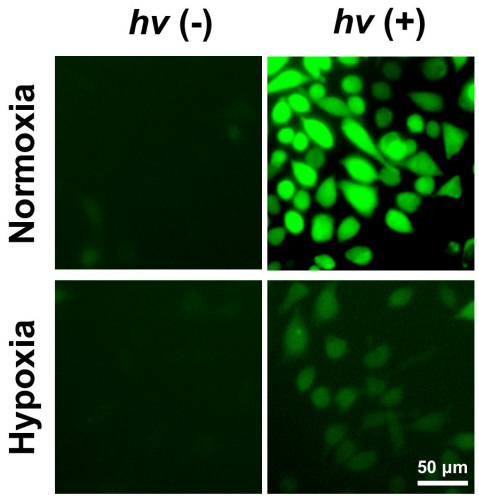

Fig. S46 Fluorescence images of HeLa cells stained with DCFH-DA (10 μM) after treatment by ^{mito}ZnPor (1 μM) under normoxia and hypoxia in the presence (+) and absence (-) of white LED light irradiation (30 mW cm^{-2}, t_{irr}= 10 min). Scale bar, 50 μm.

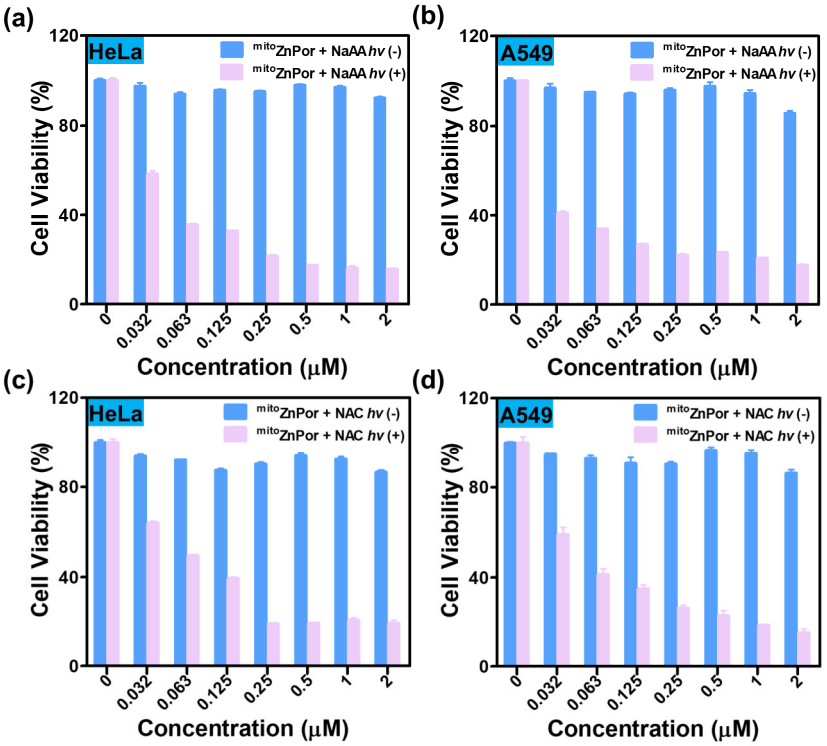

Fig. S47 Viabilities of (a) HeLa cells and (b) A549 cells treated with NaAA (1 mM) and varied concentrations of ^{mito}ZnPor (0-2 μM) in the absence and presence of white LED light irradiation (30 mW cm^{-2}, t_{irr} = 10 min) under hypoxia. Viabilities of (c) HeLa cells and (d) A549 cells treated with NAC (1 mM) and varied concentrations of ^{mito}ZnPor (0-2 μM) in the absence and presence of white LED light irradiation (30 mW cm^{-2}, t_{irr} = 10 min) under hypoxia.

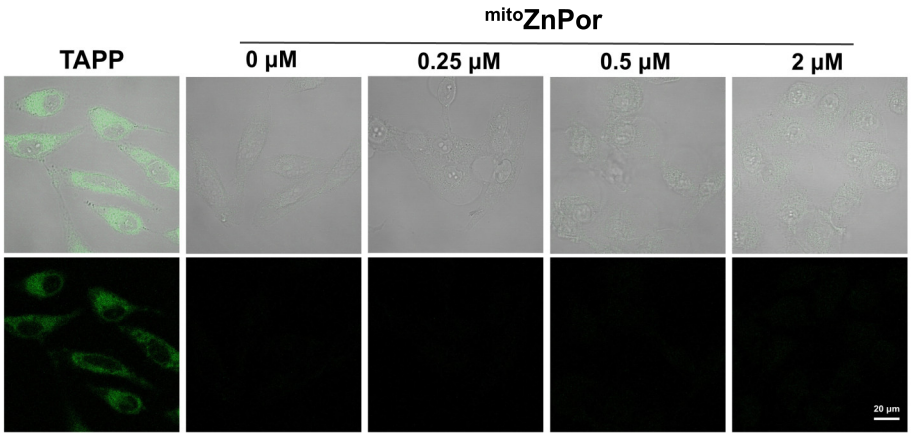

Fig. S48 CLSM images of HeLa cells stained with C11-BODIPY after treatment with ^{mito}ZnPor and photoirradiation under hypoxia. The control group was treated with TAPP (4 μM) and photoirradiation under normoxia. Scale bar, 20 μm.

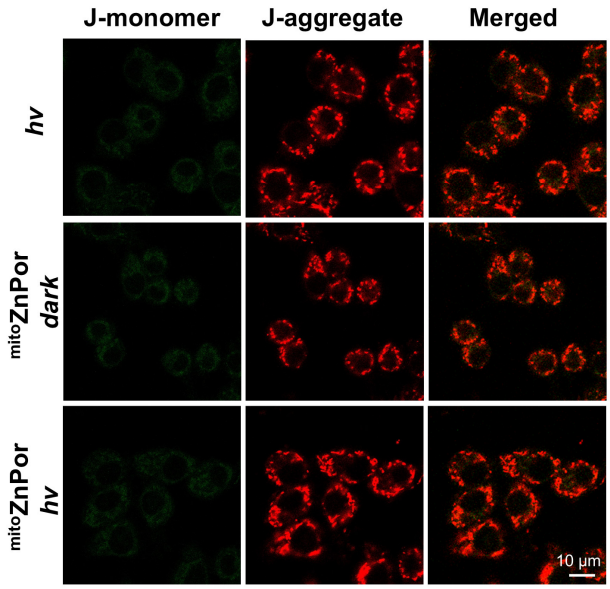

Fig. S49 CLSM images of L02 cells after treatment with ^{mito}ZnPor (1 μM) in the presence of white LED light irradiation (30 mW cm^{-2}, t_{irr} = 10 min) under hypoxia. The cells were stained with JC-1 before imaging. Scale bar, 10 μm.

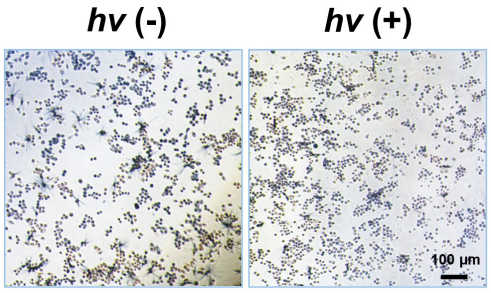

Fig. S50 Formazan formation in L02 cells after treated with 2 μM ^{mito}ZnPor in the absence and presence of white LED light irradiation (30 mW cm^{-2}, t_{irr} = 10 min) under hypoxia.

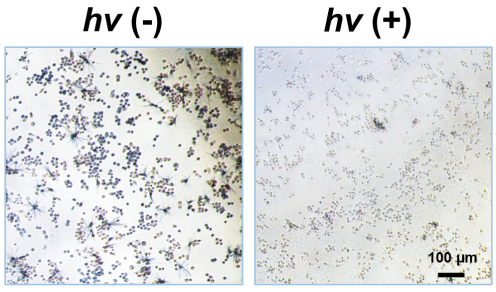

Fig. S51 Formazan formation in L02 cells after treated with 1 mM NADH and 2 μM ^{mito}ZnPor in the absence and presence of white LED light irradiation (30 mW cm^{-2}, t_{irr} = 10 min) under hypoxia.

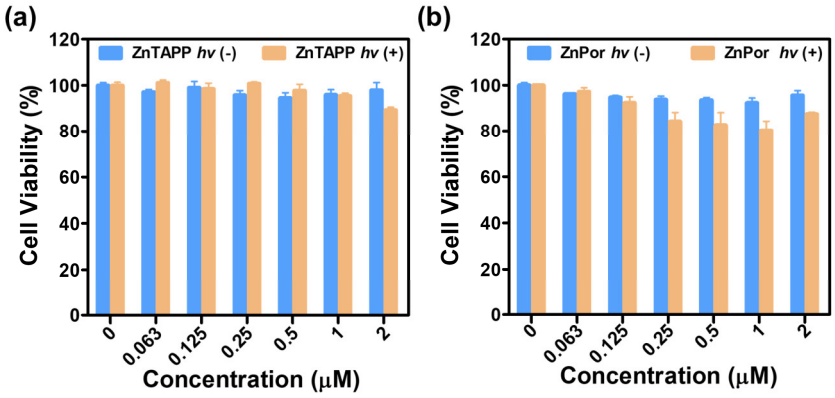

Fig. S52 (a) Viabilities of A549 cells treated with varied concentrations of ZnTAPP (0-2 μM) after white LED light irradiation (30 mW cm^{-2}, t_{irr} = 10 min) under hypoxia. (b) Viabilities of HeLa cells treated with varied concentrations of ZnPor (0-2 μM) after white LED light irradiation (30 mW cm^{-2}, t_{irr} = 10 min) under hypoxia.

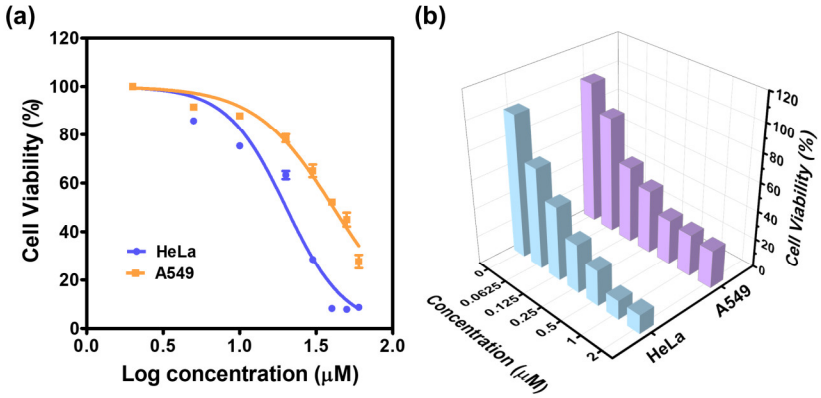

Fig. S53 (a) Viabilities of HeLa and A549 cells treated with varied concentrations of ^{mito}Por (0-60 μM) under hypoxia in the dark. (b) Viabilities of HeLa and A549 cells treated with varied concentrations of ^{mito}Por (0~2 μM) after white LED light irradiation (30 mW cm^{-2}, t_{irr} = 10 min) under hypoxia.

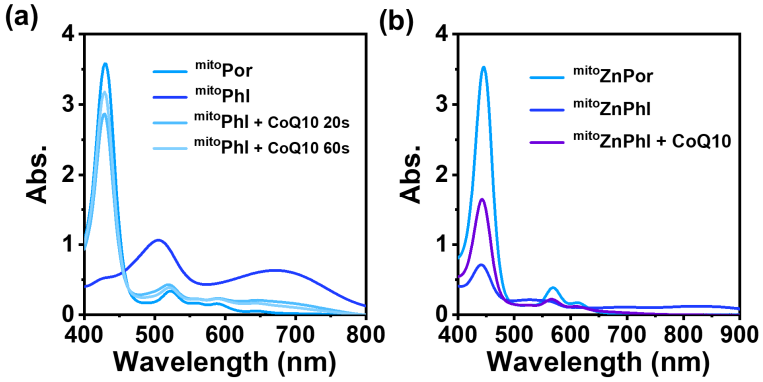

Fig. S54 (a) UV-vis spectra of solutions containing ^{mito}Phl pre and post adding CoQ10. (b) UV-vis spectra of solutions containing ^{mito}ZnPhl pre and post adding CoQ10.

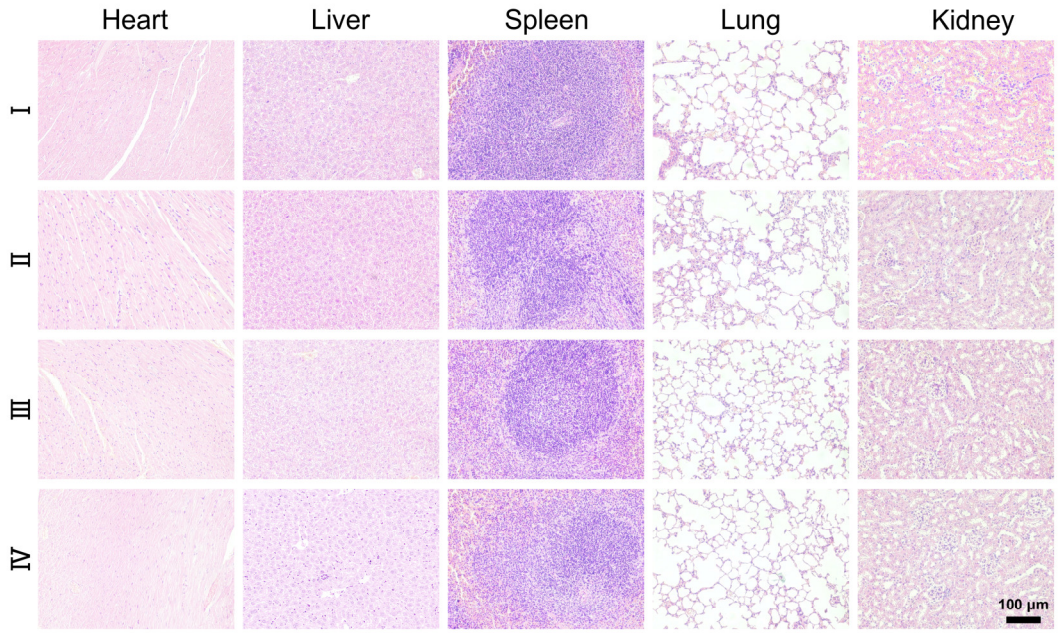

Fig. S55 H&E staining of normal organs in mice after different treatment. I: PBS, II: PBS + light, III: ^{mito}ZnPor, IV: ^{mito}ZnPor + light.

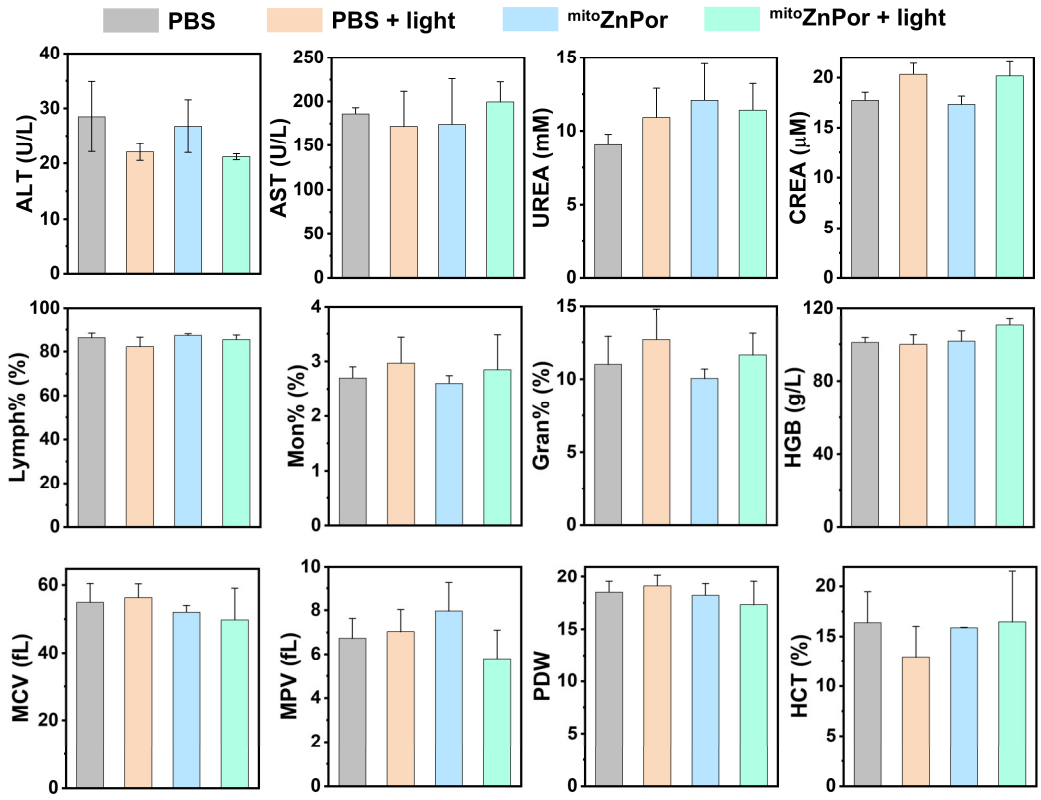

Fig. S56 Hematology markers and biochemical indexes analysis of mice in different groups.

References

1 W. Meng, B. Breiner, K. Rissanen, J. D. Thoburn, J. K. Clegg and J. R. Nitschke, *Angew. Chem. Int. Ed.*, 2011, **50**, 3479-3483.

2 M. Li, K. H. Gebremedhin, D. Ma, Z. Pu, T. Xiong, Y. Xu, J. S. Kim and X. Peng, *J. Am. Chem. Soc.*, 2022, **144**, 163-173.

3 H. Huang, S. Banerjee, K. Qiu, P. Zhang, O. Blacque, T. Malcomson, M. J. Paterson, G. J. Clarkson, M. Staniforth, V. G. Stavros, G. Gasser, H. Chao and P. J. Sadler, *Nat. Chem.*, 2019, **11**, 1041-1048.

4 H. Gong, Y. Chao, J. Xiang, X. Han, G. Song, L. Feng, J. Liu, G. Yang, Q. Chen and Z. Liu, *Nano Lett.*, 2016, **16**, 2512-2521.